Polarforschung 59 (3): 141–171, 1989 (erschienen 1991)

Taxonomy and Morphostructure of Late Neogene Diatoms from Maud Rise (Antarctic Ocean)

By Rainer Gersonde*

Summary: Based on light microscopic (LM) and scanning electron microscopic (SEM) observations late Neogene diatom taxa of the genera *Nitzschia*, *Rhizosolenia* and *Thalassiosira* that were recovered during RV „Polarstern" cruise ANT IV/4 with gravity and piston corers on the Maud Rise (SE Weddell Sea) are described and discussed. Five *Nitzschia* species (*N. arcula*, *N. aurica*, *N. barronii*, *N. lacrima*, *N. praecurta*), two *Thalassiosira* species (*T. complicata*, *T. inura*), and *Rhizosolenia costata* are described new. Some of the treated taxa are useful stratigraphic markers. Their stratigraphic range in the southern high-latitudes is described and their significance for paleoceanographic reconstructions is briefly discussed.

Zusammenfassung: Gestützt auf lichtmikroskopische (LM) und rasterelektronenmikroskopische (REM) Untersuchungen werden Diatomeentaxa der Gattungen *Nitzschia*, *Rhizosolenia* und *Thalassiosira* aus dem jüngeren Neogen beschrieben und diskutiert. Das Material wurde während der Expedition ANT IV/4 mit FS „Polarstern" im Bereich der Maud Kuppe mit Hilfe von Kolben- und Schwereloten gewonnen. Fünf *Nitzschia*-Arten (*N. arcula*, *N. aurica*, *N. barronii*, *N. lacrima*, *N. praecurta*), zwei Thalassiosira-Arten (*T. complicata*, *T. inura*) sowie *Rhizosolenia costata* werden neu beschrieben. Eine Reihe dieser Arten können als biostratigraphische Leitarten genutzt werden. Ihre stratigraphischen Reichweiten in südlichen hohen Breiten und ihre Bedeutung für paläozeanographische Rekonstruktionen wird beschrieben und kurz diskutiert.

1. INTRODUCTION

Pioneer studies on marine fossil and subfossil diatoms from the southern high-latitude Ocean were accomplished by HEIDEN & KOLBE (1928), and JOUSÉ et al. (1962) on surface sediment samples recovered in the Indian sector of the Antarctic Ocean. In 1970 DONAHUE submitted a PhD-dissertation on the paleoclimatic significance of Pleistocene diatoms from high-latitudes of the Pacific Ocean including a serie of species descriptions with photographic documentations. Unfortunately these descriptions were never published, nor were holotypes or type levels defined. Thus, according to the rules of the International Code of Botanical Nomenclature (GREUTER et al. 1988) these descriptions are not valid. More comprehensive investigations on the taxonomy of marine Neogene and Quaternary diatoms from the Southern Ocean were included by MCCOLLUM (1975), SCHRADER (1976), GOMBOS (1977), CIESIELSKI (1983), and GOMBOS & CIESIELSKI (1983) in their primarily biostratigraphically orientated studies on Deep Sea Drilling Project (DSDP) cores. Especially SCHRADER (1976) contributed to the knowledge of Neogene diatom taxa from the Antarctic Ocean by describing 24 well-documented new taxa, and by illustrating a number of undescribed forms. More specialized contributions by GOMBOS (1974), BRADY (1977), and HENDEY (1981) focused at the description and the documentation of Neogene Antarctic diatom taxa. Recent studies of sediment cores recovered during Ocean Drilling Program (ODP) Legs in the Southern Ocean that were accomplished by GERSONDE (1990) on Leg 113 material, and by BALDAUF & BARRON (in press) on Leg 119 sections, resulted in the description of new Neogene diatom taxa ranging in the Miocene.

The present study is focused at the description and documentation of diatom taxa occurring in late Neogene sediment cores that were recovered in 1986 during expedition ANT IV/4 with RV „Polarstern". The investigated sample material originates in cores, which were gathered on Queen Maud Rise, an isolated topographic elevation located in the deep sea area off Dronning Maud Land and covered by pelagic Cenozoic sediments. In 1987 these sediments were cored successfully at two sites (Sites 689 and 690) during ODP Leg 113 with the drillship „JOIDES Resolution" (BARKER, KENNETT et al. 1988). The well-preserved sediment sections gathered during Leg 113 allowed the establishment of an integrated diatom and geomagnetic stratigraphy for the Neogene time period (GERSONDE & BURCKLE 1990, GERSONDE et al. 1990). Based on the integrated stratigraphy Neogene diatom species ranges could be accurately tied to the geomagnetic time scale. Some of the taxa newly described or documented in the present paper are used as important stratigraphic marker species and are nominate species

*Dr. Rainer Gersonde, Alfred Wegener Institute for Polar and Marine Research, Columbusstraße, D-2850 Bremerhaven, Germany
Manuscript received: 08. 08. 1990; accepted: 15. 09 1990

of diatom zones established by GERSONDE & BURCKLE (1990), e.g. *Nitzschia barronii* sp. nov. and *Thalassiosira inura* sp. nov.. The stratigraphic ranges, the first appearance datum (FAD) and last appearance datum (LAD), and the paleoceanographic significance of the studied taxa is presented and summarized in this paper (Fig. 1).

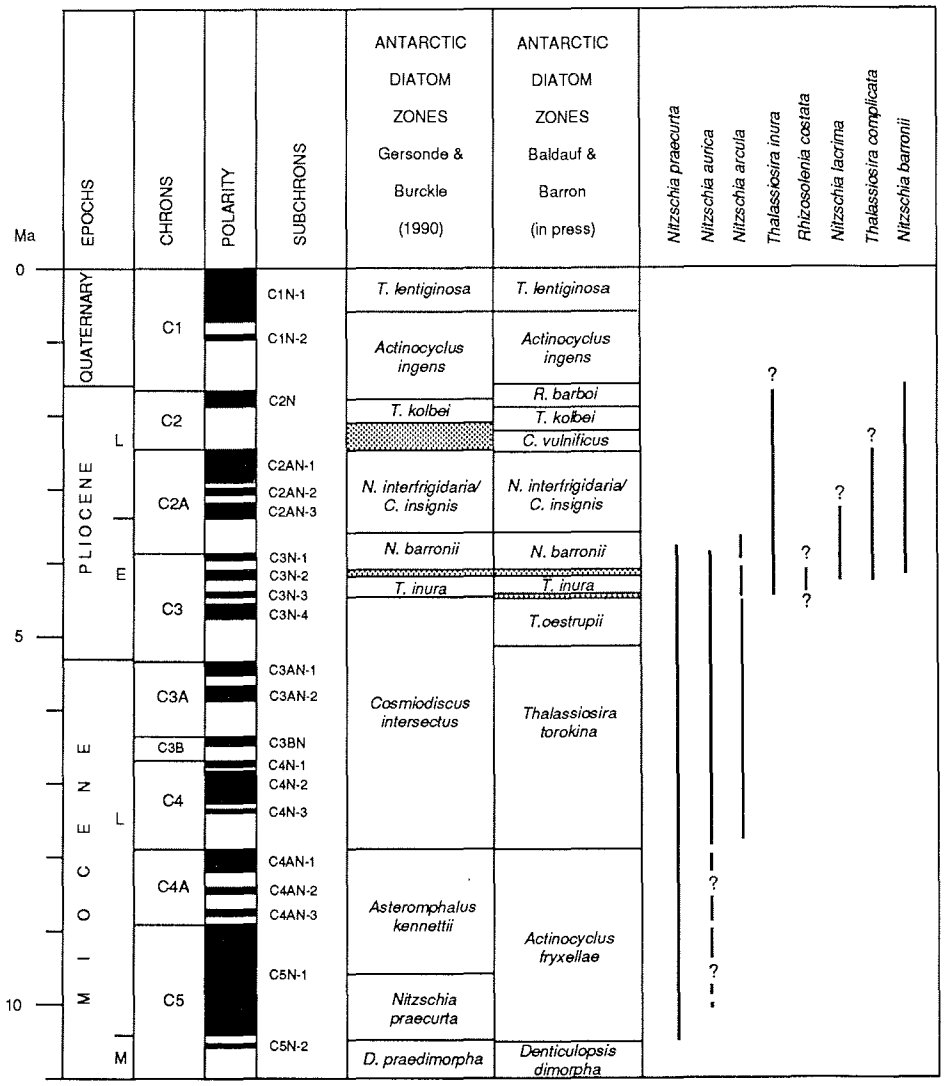

Fig. 1: Stratigraphic range of discussed taxa, correlated with the geomagnetic time scale and the Neogene diatom zonations proposed by GERSONDE & BURCKLE (1990) and BALDAUF & BARRON (in press). Stippled boxes indicate the range of uncertain age assignment for zonal boundaries. The geomagnetic time scale and absolute ages are from BERGGREN et al. (1985) and the nomenclature of geomagnetic events follows that of SPIESS (1990).

Abb. 1: Stratigraphische Reichweiten der diskutierten Taxa und deren Zuordnung zur geomagnetischen Zeitskala und den von GERSONDE & BURCKLE (1990) und BALDAUF & BARRON (im Druck) vorgeschlagenen neogenen Diatomeenzonierungen. Gerasterte Abschnitte zeigen nicht eindeutig festlegbare Zonengrenzen an. Die geomagnetische Zeitskala und die absoluten Alter sind aus BERGGREN et al. (1985). Die Nomenklatur der geomagnetischen Ereignisse folgt der von SPIESS (1990).

2. MATERIAL AND METHODS

The material used for the present study originates in two sediment cores. Core PS1458-2 was recovered with a gravity core at 65°59.34'S, 1°51.54´E at a water depth of 2487 m. The core has a length of 5.22 m and penetrates at its base upper lower Pliocene sediments (*Nitzschia interfrigidaria/Cosmiodiscus insignis* diatom Zone, Fig. 1). Piston core PS1467-1 was gathered at 64°06.51´S, 1°18.36´E in 3550 m of water. The core length is 10.99 m. The core interval between 1.6 mbsf (meters below sea floor) and the core base covers a time interval ranging in the early Pliocene (upper *Cosmiodiscus intersectus* to lowermost *Nitzschia interfrigidaria/Cosmiodiscus insignis* Zone, Fig. 1). For further stratigraphic details of the cores the reader is referred to ABELMANN et al. (1990).

The cleaning of the sediment samples, preparation of permanent mounts (using the resin Mountex, nd = 1,67) for light microscopy (LM) and scanning electron microscopy (SEM) investigations were accomplished according to the methods described by ABELMANN et al. (in prep.). Light microscopical investigations were made with a Leitz Orthoplan microscope with apochromatic optics. Micrographs were made with an automatic Leitz Orthomat camera. The scanning electron microscope investigations were completed with a Philips SEM 515.

Measurements of the diatom valve structure and the terminology for the siliceous components follows the suggestions given by ANONYMUS (1975) and ROSS et al. (1979). For the description of one *Rhizosolenia* species an amended terminology proposed by SUNDSTRÖM (1986) is used. Types were marked on LM-slides with a diamond marker and are deposited at the Friedrich-Hustedt Diatom Collection at the Alfred Wegener Institute for Polar and Marine Research, Bremerhaven.

3. DESCRIPTION OF DIATOM TAXA

Genus *Nitzschia* Hassall

A comprehensive study of the taxonomy and morphology of the genus *Nitzschia* was achieved by Hasle (1964, 1965a, b), based on extensive light and electron microscope investigations.

Nitzschia arcula sp. nov.

(Pl. 2, Fig. 4; Pl. 4, Fig. 4; Pl. 5, Figs. 1-6)

Description: Valve linear oblong, isopolar. Apices obtusely rounded. Apical axis 15 - 43 µm, transapical axis 3. 5 - 8 µm (Fig. 2). Transapical interstriae generally straight and heavily silicified (Pl. 2, Fig. 4). Interstriae next to apices slightly curved and branched towards the apices, 8 - 14 interstriae in 10 µm (Fig. 3). Striae with two or three rows of regular to irregular spaced poroids (32 - 40 in 10 µm) (Pl. 4, Fig. 4). Raphe, located in the junction between valve face and mantle. Central nodule absent (Pl. 4, Fig. 4). Generally number of fibulae as number of

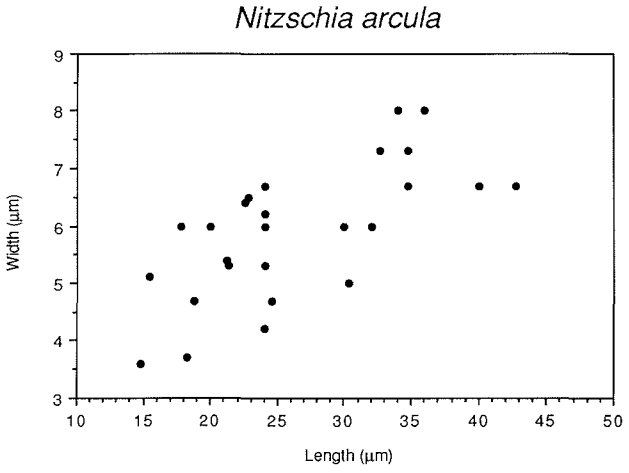

Fig. 2: Length - width ratio of *Nitzschia arcula*.

Abb. 2: Längen/Breiten-Verhältnis von *Nitzschia arcula*.

interstriae, or inconsiderably greater (Pl. 2, Fig. 4) .
Holotype: Deposited in the Friedrich-Hustedt Collection No. Zu 4/3 (Pl. 5, Fig. 1).
Type locality: Core PS1467-1, Maud Rise, southeast Weddell Sea.
Type level: Marine early Pliocene, Sample PS1467-1, 804 cm.
Paratype: Deposited in the Friedrich-Hustedt Collection No. Zu 4/3 (Pl. 5, Fig. 3) from Sample PS1467-1, 804 cm.
Stratigraphic occurrence: In the *Cosmiodiscus intersectus, Thalassiosira inura* and the lower portion of the *Nitzschia barronii* diatom Zones (late late Miocene to early Pliocene, Fig. 1) (GERSONDE & BURCKLE 1990).
Derivation of name: arcula (Latin) = small box.

Discussion and remarks: *N. arcula* differs from the Pliocene species *N. pseudocylindrica* Schrader described from the Norwegian Sea area (in SCHRADER & FENNER 1976, p. 992, pl. 1, figs. 3 -5, 12, 15-18) by its more heavily silicified interstriae and the strial structure. The striae of *N. pseudocylindrica* consist of one row of poroids. *N. arcula* differs from *N. cylindrus* (Grun.) Hasle (description in HASLE 1965b, p. 34, pl. 12, figs. 6 - 12; pl. 14, figs. 1 -10; pl. 17, figs. 2 - 4 as *Fragilariopsis cylindrus*) by its coarser valve interstrial and strial structure. *N. arcula* differs from *N. linearis* (Castr.) Hasle (description in HASLE 1965b, p. 37, pl. 12, fig. 17; pl. 15, figs. 9 - 11 as *Fragilariopsis linearis*) by its generally smaller valve length and its more delicate strial and interstrial structure.

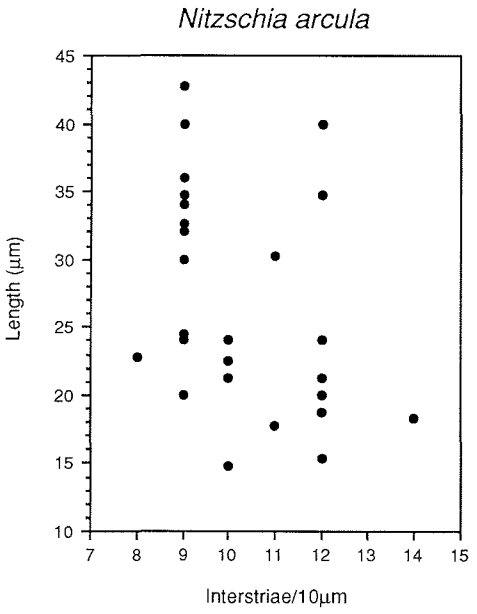

Fig. 3: Correlation between valve length and number of interstriae in 10 µm of *Nitzschia arcula*.

Abb. 3: Korrelation zwischen Schalenlänge und Anzahl der Interstriae in 10 µm von *Nitzschia arcula*.

Nitzschia aurica sp. nov.
(Pl. 1, Figs. 18 - 25; Pl. 3, Fig. 5; Pl. 4, Figs. 5, 6; Pl. 7, Fig. 6)
Description: Valve broadly elliptical to subcircular, isopolar, few specimen very slightly heteropolar. Apices broadly rounded. Apical axis 7 - 31 µm, transapical axis 4.5 - 10 µm, length and width positively correlated (Fig. 4). Transapical interstriae straight in the middle portion of valve face and distinctly curved towards the apices, 9 - 16 in 10 µm, number of interstriae negatively correlated with valve length (Fig. 5). Interstriae next to apices branched towards apices (Pl. 4, Figs. 5, 6). Striae with one or two rows of regular to irregular spaced poroids (in general 30 - 40 in 10 µm), in the median area of the valve often discontinuous, leading to small hyaline fields (Pl. 4, Figs. 5, 6). Raphe eccentric, located in the junction between valve face and mantle. Central nodule absent (Pl. 7, Fig. 6). Number of fibulae as number of interstriae or slightly smaller. Near apices often number of interstriae greater than number of fibulae.

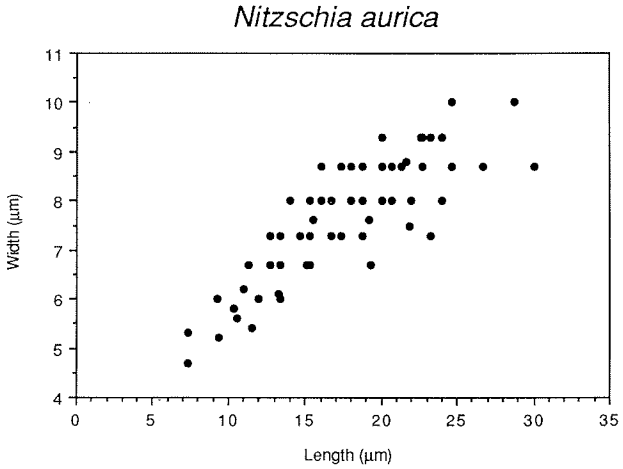

Fig. 4: Length - width ratio of *Nitzschia aurica*.

Abb. 4: Längen/Breiten-Verhältnis von *Nitzschia aurica*.

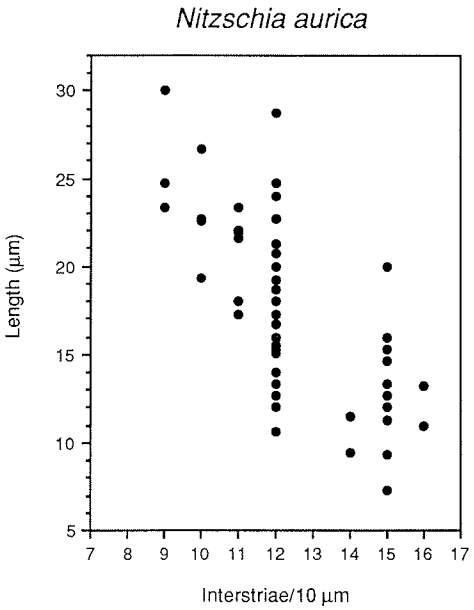

Fig. 5: Correlation between valve length and number of interstriae in 10 µm of *Nitzschia aurica*.

Abb. 5: Korrelation zwischen Schalenlänge und Anzahl der Interstriae in 10 µm von *Nitzschia aurica*.

Holotype: Deposited in the Friedrich-Hustedt Collection No. Zu 4/3 (Pl. 1, Fig. 19).
Type locality: Core PS1467-1, Maud Rise, southeast Weddell Sea.
Type level: Marine early Pliocene, Sample PS1467-1, 804 cm.
Paratype: Deposited in the Friedrich-Hustedt Collection No. Zu 4/3 (Pl. 1, Fig. 20) from Sample PS1467-1, 804 cm.
Stratigraphic occurrence: Trace in the *Nitzschia praecurta* and *Asteromphalus kennettii* diatom Zones (early late Miocene) and consistent in the *Cosmiodiscus intersectus, Thalassiosira inura* and the lower portion of the *Nitzschia barronii* diatom Zones (late late Miocene to early Pliocene, Fig. 1) (GERSONDE & BURCKLE 1990).
Derivation of name: After my daughter Aurica.

Discussion and remarks: *N. aurica* is distinct from *N. praecurta* by its elliptical to subcircular valve shape. Both species have similiar stratigraphic ranges (Fig. 1) but their abundance pattern is different (GERSONDE &

BURCKLE 1990). *N. aurica* has affinities to *N. porteri* Frenguelli (FRENGUELLI 1949, p. 116, pl. 1, figs. 33, 34) described from Neogene sediments in Chile. According to the description and the given two figures *N. porteri* is larger in size (length 25 - 37 µm, width 10 - 11 µm), the apices are more acute, the interstriae are less silicified and the interstriae next to apices are not distinctly branched towards the apices, compared with *N. aurica*. Unfortunately no original Frenguelli material from Tiltil y Mejillones is available so that the description of FRENGUELLI (1949) cannot be scrutinized. *N. aurica* differs from *N. pseudonana* Hasle (HASLE 1965b, p. 22, pl. 1, figs. 7 - 14; pl. 4, figs. 20, 21; pl. 8, figs. 1 - 9; pl. 17, fig. 6 as *Fragilariopsis pseudonana*, for validation of this taxon see HASLE 1974, p. 425 - 428) and from *N. cylindroformis* Hasle (HASLE & BOOTH 1984, p. 493, figs. 1 - 22, 24, 27, 28, 32 - 36, 41, 44) by its coarser interstrial and strial structure.

Nitzschia barronii sp. nov.

(Pl. 3, Fig. 6; Pl. 4, Figs. 1 - 3; Pl. 5, Figs. 7 - 17)

Fragilariopsis lanceolata nom. nud. DONAHUE 1970, p. 190, pl. 7, figs. m-p

Nitzschia angulata auct. non (O'Meara) Hasle, BARRON 1985, p. 267, fig. 14.13,14

Description: Valve outline variable elliptical to rhombic, isopolar or slightly heteropolar. Heteropolar specimen tapering more to one apex. Apical axis 13 - 52 µm, transapical axis 6 - 17 µm at widest point. Length and width positively correlated, length/width ratio in average 2.3 (Fig. 6). Transapical interstriae heavily silicified, straight to slightly oblique in middle of valve face and curved towards the apices, 7 - 11 in 10 µm. Number of interstriae in 10 µm and negatively correlated with valve length (Fig. 7). Striae in apical sectors of valve face with two rows of regular spaced poroids (in general 17 - 18 in 10 µm, total range 13 - 26 in 10 µm) located close to interstriae (Pl. 4, Figs. 1 - 3). Striae in central part of valve face with one or two rows of regular to irregularly spaced poroids, often discontinuous, leading to hyaline, non-perforated fields (Pl. 3, Fig. 6; Pl. 4, Fig. 2). Raphe eccentric, located in the junction between valve face and valve mantle. Valve mantle low, hyaline. Central nodule absent (Pl. 4, Fig. 1). Number of fibulae as number of interstriae or inconsiderably smaller.

Holotype: Deposited in the Friedrich-Hustedt Collection No. Zu 4/7 (Pl. 5, Fig. 14).

Type locality: Core PS1467-1, Maud Rise, southeast Weddell Sea.

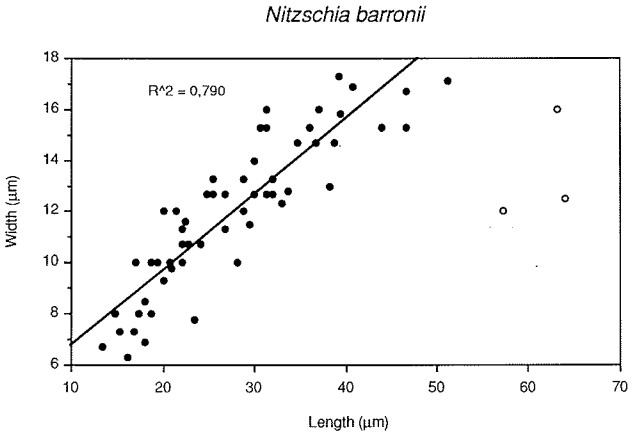

Fig. 6: Length - width ratio of *Nitzschia barronii* (black dots) and *Nitzschia* sp. A. (open dots).

Abb. 6: Längen/Breiten-Verhältnis von *Nitzschia barronii* (geschlossene Kreise) und *Nitzschia* sp. A. (offene Kreise).

Type level: Marine early Pliocene, Sample PS1467-1, 200 cm.

Paratype: Deposited in the Friedrich-Hustedt Collection No. Zu 4/6 (Pl. 5, Fig. 13) from Sample PS1467-1, 200 cm.

Stratigraphic occurrence: Nominate species of the early Pliocene *N. barronii* diatom Zone of GERSONDE & BURCKLE (1990). FAD, at ca. 4.2 - 4.1 Ma, defines the base of the *N. barronii* diatom Zone; LAD in the lower portion of the *Actinocyclus ingens* Zone (early Pleistocene, Fig. 1) (GERSONDE & BURCKLE 1990, BALDAUF & BARRON in press).

Derivation of name: Dedicated to Dr. John A. Barron, paleontologist and stratigrapher at the U.S. Geological Survey, Menlo Park, California.

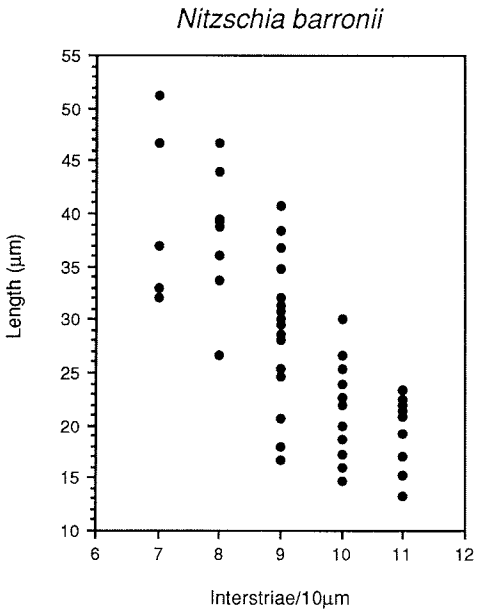

Fig. 7: Correlation between valve length and number of interstriae in 10 µm of *Nitzschia barronii*.

Abb. 7: Korrelation zwischen Schalenlänge und Anzahl der Interstriae in 10 µm von *Nitzschia barronii*.

Discussion and remarks: *Nitzschia barronii* has affinities to *Nitzschia angulata* (O´Meara) Hasle considering the valve outline and the arrangement of the interstriae (for a comprehensive description of *N. angulata*, syn. *Fragilariopsis rhombica* see HASLE 1965b, p. 24). *N. barronii* differs from *N. angulata* by its distinct coarser strial structure and the presence of hyaline, non-perforated areas on the valve face.

Both, *N. angulata* and *N. barronii* are endemic to the Southern Ocean. However, while *N. angulata* is a prominent extant species, *N. barronii* is extinct. Probably *N. barronii* is a phylogenetic precursor of *N. angulata*. However, a phylogenetic transition between both taxa could not yet be documented.

Another taxon close to *N. barronii* is *Nitzschia* sp. A (Pl. 5, Fig. 21). This heteropolar taxon differs from *N. barronii* by its valve shape: the more lanceolate outline and a length/width ratio > 4.0 (Fig. 6). Its apical interstriae are less curved. *Nitzschia* sp. A will be described in more detail in a separate paper.

N. barronii is probably conspecific with *N. angulata*, the nominate species of the *N. angulata* diatom Zone defined by WEAVER & GOMBOS (1981). Unfortunately WEAVER & GOMBOS did not photographically document the species, nor was this done by CIESIELSKI (1983), who also used the FAD of a *N. angulata*. In a compilation of Neogene diatom biostratigraphies and biostratigraphic marker species BARRON (1985) labels a species as *N. angulata* which, based on its photographically documented outline (fig. 14.13, 14 in BARRON, 1985), is conspecific with *N. barronii*.

In ODP Leg 113 Holes 689B and 690B drilled on Maud Rise the FAD of *N. barronii* is correlated to the lower part of the geomagnetic Subchron C3N-2 (ca. 4.2 Ma). At the same age it was also found in piston core PS1467-1. However, at ODP Leg 113 Holes 695A and 697B, drilled southeast of the South Orkney Islands, the FAD of *N. barronii* is correlated to the top of Subchron C3N-2 (4.1 Ma) (GERSONDE & BURCKLE 1990). Also WEAVER & GOMBOS (1981) place the FAD of their *N. angulata* (=? *N. barronii*) at the top of Subchron C3N-2. CIESIELSKI (1983) notes that the FAD of *N. angulata* (=? *N. barronii*) is diachronous and ranges within Subchron C3N-2 from about 4.2 to 4.1 Ma. He states however, that in most of his cores the FAD is at about 4.2 Ma. Also BALDAUF & BARRON (in press) place the FAD of *N. barronii* at 4.2 Ma, based on the study of ODP Leg 119 holes drilled in the Indian sector of the Southern Ocean, south of the present Antarctic Polar Front.

Nitzschia lacrima sp. nov.

(Pl. 1, Fig. 1-6, 26; Pl. 2, Figs. 1 - 3)

Description: Valve clavate. One apex more broadly rounded and the other one tapering to an acutely rounded tip. Apical axis 21 - 60 µm, transapical axis 7 - 12 µm at widest point. Transapical interstriae straight in middle of valve face and slightly curved towards the apices, 10 - 12 in 10 µm. Interstria close to broadly rounded apex branched towards apex. Striae with one or two rows of poroids (ca. 40 in 10 µm) intermitted by regular spaced and apically oriented thickenings (11 - 12 in 10 µm) (Pl. 2, Figs. 1, 2). Raphe eccentric, located in the junction between valve face and valve mantle. Central nodule absent (Pl. 1, Fig. 26; Pl. 2, Fig. 1). Number of fibulae as number of interstriae.

Holotype: Deposited in the Friedrich-Hustedt Collection No. Zu 4/5 (Pl. 1, Figs. 2, 3).

Type locality: Core PS1467-1, Maud Rise, southeast Weddell Sea.

Type level: Marine early Pliocene, Sample PS1467-1, 866 cm.

Paratypes: Deposited in the Friedrich-Hustedt Collection No. Zu 4/5 (Pl. 1, Figs. 1, 4), from Sample PS1467-1, 866 cm.

Stratigraphic occurrence: In the *Thalassiosira inura* and *Nitzschia barronii* diatom Zones and the lower portion of the *Nitzschia interfrigidaria/Cosmiodiscus insignis* Zone (early Pliocene, Fig. 1) (GERSONDE & BURCKLE 1990).

Derivation of name: lacrima (Latin) - tear.

Discussion: Another calvate-shaped *Nitzschia* taxon is *N. clementia* Gombos (1977, p., pl. 8, Figs. 18, 19) that occurs in the late Miocene to early Pliocene of the Southern Ocean (GOMBOS 1977, GERSONDE & BURCKLE 1990). *N. lacrima* is disctinct from *N. clementia* by its coarser strial structure.

Nitzschia praecurta sp. nov.

(Pl. 1, Figs. 7 - 17; Pl. 2, Fig. 5, 6; Pl. 3, Fig. 3, 4; Pl. 10, Fig. 7)

? *Nitzschia* sp. 14, SCHRADER 1976, pl. 2, figs. 8, 36.

Description: Valve linear-oblong, isopolar to very slightly heteropolar. Apices broadly rounded. Apical axis 8 - 42 µm, transapical axis 3.3 - 8.3 µm (Fig. 8). Transapical interstriae straight in the middle portion of valve face and curved towards the apices, generally 10 - 15 in 10 µm (Fig. 9). Interstriae next to the apices branched towards apex. Striae with one or two rows of regular to irregular spaced poroids (27 - 35 in 10 µm), in the median area of the valve often discontinuous, leading to hyaline, non-perforated fields (Pl. 2, Figs. 5, 6; Pl. 3, Figs. 3, 4; Pl. 10, Fig. 7). Raphe eccentric, located in the junction between valve face and mantle. Central nodule absent (Pl. 3, Fig. 3). In median part of valve number of fibulae as number of interstriae or slightly smaller. Near apices number of interstriae often greater than number of fibulae.

Holotype: Deposited in the Friedrich-Hustedt Collection No. Zu 4/4 (Pl. 1, Fig. 11).

Type locality: Core PS1467-1, Maud Rise, southeast Weddell Sea.

Type level: Marine early Pliocene, Sample PS1467-1, 790 cm.

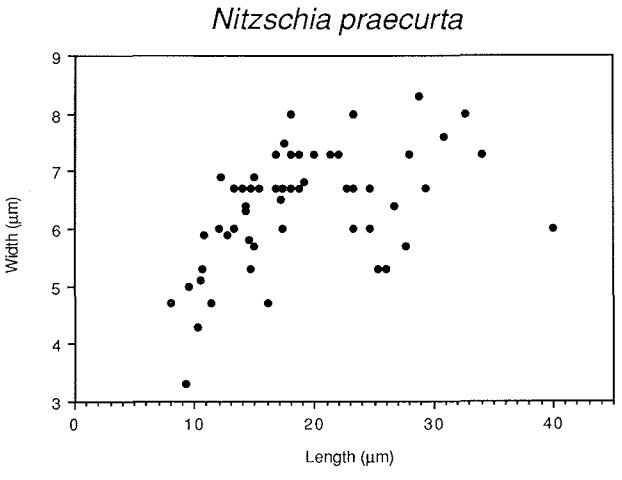

Fig. 8: Length - width ratio of *Nitzschia praecurta*.

Abb. 8: Längen/Breiten-Verhältnis von *Nitzschia praecurta*.

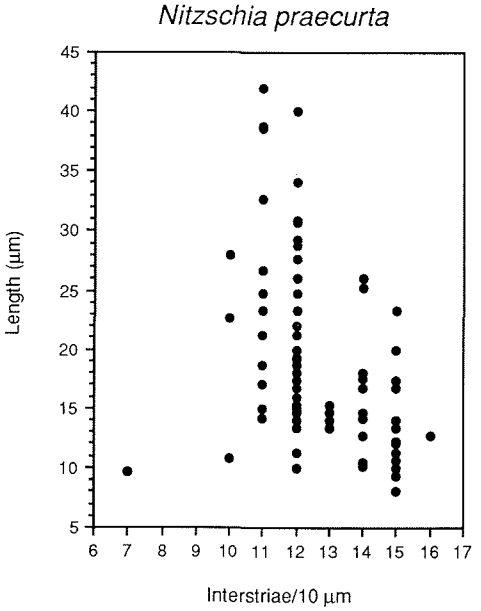

Fig. 9: Correlation between valve length and number of interstriae in 10 µm of *Nitzschia praecurta*.

Abb. 9: Korrelation zwischen Schalenlänge und Anzahl der Interstriae in 10 µm von *Nitzschia praecurta*.

Paratype: Deposited in the Friedrich-Hustedt Collection'No. Zu 4/4 (Pl. 1, Fig. 10), from Sample PS1467-1, 790 cm.

Stratigraphic occurrence: Nominate species of the early late Miocene *N. praecurta* diatom Zone of GERSONDE & BURCKLE (1990). FAD at ca. 10.5 Ma, defines base of the *N. praecurta* diatom Zone; LAD in the *Nitzschia barronii* Zone (early Pliocene, Fig. 1)(GERSONDE & BURCKLE 1990).

Discussion and remarks: *N. praecurta* is distinct from *N. aurica* by its linear-oblong valve shape. Very probably *N. praecurta* is conspecific with a taxon labeled *Nitzschia* sp. 14 (SCHRADER 1976, pl. 2, figs. 8, 36). *N. praecurta* has affinities to *N. curta* (v.Heurck) Hasle and *N. linearis* (Castr.) Hasle, two prominent extant species endemic to the Antarctic Ocean. Descriptions of these taxa are in HASLE (1965b, p. 32, pl. 6, fig. 6; pl. 12, figs. 2 - 5; pl. 13, figs. 1 -6; pl. 16, fig. 6; pl. 17, fig. 5 as *Fragilariopsis curta*, and p. 37, pl. 12, fig. 17; pl. 15, figs. 9 -11 as *Fragilariopsis linearis*). *N. praecurta* differs from *N. curta* by the less expressed heteropolarity and the more broadly rounded apices. *N. praecurta* is distinct from *N. linearis* by its shorter length and more delicate strial/ interstrial structure. Probably *N. praecurta* is a phylogenetic precursor of *N. curta or N. linearis*. However, a phylogenetic transition between *N. praecurta* and one of the extant taxa could not yet be documented.

Genus *Rhizosolenia* Brightwell

A modern revision of the taxonomy of *Rhizosolenia* was accomplished by SUNDSTRÖM (1986). In this monograph an emended diagnosis of *Rhizosolenia*, emended circumscriptions comprising 24 *Rhizosolenia* species, five new species and four infraspecific taxa were proposed.

Rhizosolenia costata sp. nov.

(Pl. 9, Figs. 1 - 6; Pl. 10, Figs. 1 - 6)

Description: Valve circular, apical portion of valve conoidal-cylindrical, central and basal part conoidal enlarged. Apical portion of valve and process heavily silicified, central and basal part more weakly silicified. Valve perforated by areolae arranged in radially oriented striae (ca. 9 - 24 striae /10 µm). Length of individual striae irregular. Arrangement of areolae not regular in apical portion of valve (Pl. 10, Figs. 3 -5), more regular in central and basal part (Pl. 3, Figs. 1, 2), ca. 14 - 19 areolae in 10 µm. Vela were not observed. Valve ornamented by radially oriented costae, irregular in length. Costae strongly silicified and wall-like in conoidal-cylindrical apical portion of valve, less developed in central and basal part (Pl. 10, Figs. 1, 2). Apical end of costa wall broadly rounded (Pl. 10, Figs. 1, 3 - 5). Costae wall may be strutted by tangentially oriented thickenings (Pl. 10, Figs. 4,

5). Generally only heavily silicified apical portion of valve and process preserved. Length of only encountred specimen with preserved basal part of valve is 125 µm (Pl. 10, Fig. 1). Contiguous area not observed. Process 18 - 29 µm in length, heavily silicified, slightly tapering from base with rounded tip. Process with internal lumen, length ca. 1/3 of process length, broad in basal part (Pl. 9, Fig. 3), tapering into narrow canal that opens at tip (Pl. 9, Fig. 2). A labiate structure could not be observed at connection between lumen and valve interior. No girdles were observed.
Holotype: Deposited in the Friedrich-Hustedt Collection No. Zu 4/8 (Pl. 9, Figs. 1-3).
Type locality: Core PS1467-1, Maud Rise, southeast Weddell Sea.
Type level: Marine Pliocene, Sample PS1467-1, 970 cm.
Paratype: Deposited in the Friedrich-Hustedt Collection No. Zu 4/8 (Pl. 9, Figs. 4 -6) from Sample PS1467-1, 970 cm.
Stratigraphic occurrence: In the early Pliocene *Nitzschia barronii* and *Thalassiosira inura* diatom Zones that range from 4.47 to 3.6 Ma (GERSONDE & BURCKLE 1990) (Fig. 1).
Derivation of name: costa (Latin) = rib.

Discussion and remarks: The costae of the described species are probably structures close to otaria, which are typical apical structures of a number of *Rhizosolenia* species, such as *R. styliformis* Brightwell, *R. polydactyla* Castracane, *R. borealis* Sundström, and *R. sima* Castracane (also compare SUNDSTRÖM 1986). However, a true otarium is a regular structure that occurs as a pair, located nearly opposite to each other, according to ROSS et al. (1979). More irregular occuring apical thickenings of the valve were reported from the infraspecific taxa, *R. polydactyla* f. *squamosa* Sundström and *R. sima* f. *silicea* Sundström. Both are restricted to the southern high-latitude ocean and can be regarded as „resting spores", according to SUNDSTRÖM (1986).

Genus *Thalassiosira* Cleve

The genus *Thalassiosira* is characterized by the presence of strutted processes and areolae having external foramina and internal cribra. The strutted processes are arranged in a near-marginal ring and usually at least one near the valve center or in a ring on the valve face. Each valve has one or more labiate processes (also compare descriptions in HASLE 1973 a,b and JOHANSEN & FRYXELL 1985).

Thalassiosira complicata sp. nov.

(Pl. 3, Figs. 1, 2; Pl. 5, Figs. 18 - 20; Pl. 6, Figs. 1- 6; Pl. 7, Figs. 1 - 5)

Description: Valve disc-shaped, 16 - 65 µm in diameter, with smoothly curved shallow valve mantle and small central depression. Dense areolation at valve mantle and marginal part of valve face, 17 - 28 areolae in 10 µm, arranged in tangential rows at valve mantle and more curved rows with radial orientation in marginal part of valve face (Pl. 7, Fig. 4). Central part of valve face with areolae arranged in radial and subradial rows, 12 - 18 in 10 µm (Pl. 3, Fig. 1, 2; Pl. 5, Fig. 18; Pl. 7, Fig. 2). Marginal part of valve face separated from central part by concentric ring of strutted processes. Areolae with slender cylindriform chambers (Pl. 7, Fig. 5). Central area hyaline and sunken in, often marked by distinct circular depression (Pl. 7, Fig. 2). Valve mantle with ring of strutted processes close to valve margin. Strutted processes regularily and densely spaced (6 - 10 in 10 µm), flat on outside of valve, with internally short extensions and opercula covering the four satellite pores (Pl. 7, Fig. 3). Strutted processes of concentric ring on valve face of same structure as marginal strutted processes, less densely spaced (4 - 8 in 10 µm), each located on a radial row of areolae that extends from the margin to the central hyaline area (Pl. 7, Figs. 1, 2). Single labiate process, located near valve face margin between marginal and median rings of strutted processes. Labiate process on stalk internally, the slit being parallel or nearly parallel to the marginal tangent (Pl. 7, Fig. 1).
Holotype: Deposited in the Friedrich-Hustedt Collection No. Zu 4/7 (Pl. 6, Figs. 1-3).
Type locality: Core PS1467-1, Maud Rise, southeast Weddell Sea.
Type level: Marine Pliocene, Sample PS1467-1, 200 cm.
Paratype: Deposited in the Friedrich-Hustedt Collection No. Zu 4/7 (Pl. 6, Figs. 4, 5) from Sample PS1467-1, 200 cm.
Stratigraphic occurrence: FAD in the upper portion of the early Pliocene *Thalassiosira inura* Zone at ca. 4.3 Ma; LAD near the boundary of the late Pliocene *Nitzschia interfrigidaria/Cosmiodiscus insignis* and the *Thalassiosira kolbei* Zones at ca. 2. 5 Ma (Fig. 1) (GERSONDE & BURCKLE 1990).

Discussion and remarks: *T. complicata* has some affinities to *T. opposita* Koizumi, described from upper Miocene sediments in the northwest Pacific Ocean (KOIZUMI 1980, p. 396, pl. 1, figs. 15 - 17) in the arrangement of areolae and the marginal and median rings of strutted processes. *T. opposita* differs by the presence of two central opposite processes that are surrounded by large and conspicous areolae.

Thalassiosira inura sp. nov.
(Pl. 6, Figs. 7 - 14; Pl. 8, Figs. 1 - 6)

Cestodiscus ? sp., GOMBOS 1977, pl. 5, Fig. 8.

Description: Valve convex, depressed in the center, 12 - 30 µm in diameter. Dense areolation in marginal portion of valve, 15 - 22 areolae in 10 µm (in average 18), with mostly cylindriform chambers (Pl. 8, Fig. 6) arranged in curved rows (Pl. 8, Figs. 1, 3, 4). Marginal area of valve with cylindriform areolae distinct from median valve portion with areolae having bulbous inflated chambers (Pl. 8, Fig. 6), 8 - 14 in 10 µm, arranged in curved rows or disordered. Central area hyaline and sunken in, diameter 1/3 to 1/5 of valve diameter, marked by distinct circular depression in valve center, around 1 µm in diameter (Pl. 8, Figs. 3, 4). Valve mantle with ring of strutted processes located 2 - 3 areolae off valve margin. Strutted processes evenly spaced (3 - 4 in 10 µm), processes flat on outside of valve, with internally short extensions and opercula covering the four satellite pores (Pl. 8, Fig. 2). Single strutted process located about midway between valve center and valve margin in the area with bulbous chambered areolae (Pl. 8, Figs. 1 - 5), of same structure than marginal strutted processes. Single labiate process, located opposite to strutted process on valve face near boundary between marginal area with cylindriform areolae and median area with boulbous chambered areolae. Slit of labiate process parallel to the marginal tangent (Pl. 8, Fig. 2).

Holotype: Deposited in the Friedrich-Hustedt Collection No. Zu 4/7 (Pl. 6, Figs. 7, 8).

Type locality: Core PS1467-1, Maud Rise, southeast Weddell Sea.

Type level: Marine Pliocene, Sample PS1467-1, 200 cm.

Paratype: Deposited in the Friedrich-Hustedt Collection No. Zu 4/7 (Pl. 6, Figs. 9, 10) from Sample PS1467-1, 200 cm.

Stratigraphic occurrence: Nominate species of the early Pliocene *T. inura* diatom Zone of GERSONDE & BURCKLE (1990). FAD at 4.47 Ma, defines base of the *T. inura* diatom Zone; LAD in the lower portion of the *Actinocyclus ingens* Zone at ca. ?1.7 Ma (early Pleistocene, Fig. 1; GERSONDE & BURCKLE 1990).

Derivation of name: inuro (Latin) - flatten down.

Discussion and remarks:*T. inura* has some affinities to *T. jacksonii* Koizumi & Barron, described from upper Miocene and Pliocene sediments in the northwest Pacific Ocean (KOIZUMI 1980, p. 396, pl. 1, figs. 11 - 14) in valve size and shape, and the arrangement of areolae. *T. jacksonii* differs by its more delicate areolation and by the presence of a strutted process located in the hyaline central area according to the description given by KOIZUMI. *T. gracilis* differs from *T. inura* by the lack of a distinct hyaline central area marked by a circular depression, and by the presence of a nearly central strutted process. In their study of Neogene sediments from Leg 113 holes GERSONDE & BURCKLE (1990) could not encounter *T. gracilis* (Karsten) Hustedt in lower Pliocene sediments from the Atlantic sector of the Southern Ocean, nor was this taxon found in the early Pliocene of Core PS1467-1. It should however be stated that, similiar to *T. inura*, *T. gracilis* (Karsten) Hustedt is characterized by bulbous areola chambers in the central part of the valve and more slender, cylindriform chambers on the margin (see FRYXELL & HASLE 1979, fig. 18).

4. CONCLUSION

In the present paper eight diatom species that occur in the late Neogene of the southern high-latitude ocean are described and photographically documented by light and scanning electron microscopy. Up to now these taxa were only reported from the Antarctic Ocean, and it can be speculated that they are endemic to the southern high-latitudes. Five of the described taxa, *Nitzschia aurica, N. barronii, N. praecurta, Thalassiosira complicata,* and *T. inura*, are biostratigraphically useful species because of their consistent occurrence in late Neogene sediment sections of the Southern Ocean. The first appearance date (FAD) of *N. praecurta, N. barronii* and *T. inura* was used for the definition of the base of diatom zones by GERSONDE & BURCKLE (in press) (Fig. 1).

Five of the described species, *Nitzschia barronii*, *N. lacrima*, *Thalassiosira complicata*, *T. inura*, and *Rhizosolenia costata*, have their FAD in the early Pliocene at around 4. 5 to 4.2 Ma. This is a time interval that follows a climatic optimum in the Southern Ocean marked by the invasion of several low- and mid-latitude species into the high-latitudes of the Southern Ocean, an event which started at about 4.8 Ma (ABELMANN et al. 1990). The first appearance of a series of species that are very probably endemic to the Southern Ocean area may be indication for an increase of latitudinal thermal contrast during the late early Pliocene and the decline of surface water temperatures. Probably, the late early Pliocene extinction of *N. praecurta*, *N. aurica*, and *N. arcula*, which have their frist appearances within the late Miocene, is linked to this paleoenvironmental development.

Yet another series of diatom taxa ranging in the late Neogene of the Southern Ocean is not well described or still unknown. Further taxonomic investigation of these taxa is in progress, and their stratigraphical and paleoenvironmental significance is under study.

5. ACKNOWLEDGMENT

The author is grateful to Grethe R. Hasle, Greta A. Fryxell, and Andrea Abelmann for critical review of the manuscript. I also thank Ruth Cordelair and Ute Bock for laboratory assistance. This work was supported by the Deutsche Forschungsgemeinschaft. This is Alfred Wegener Institute contribution No. 276.

References

Abelmann, A., Gersonde, R. & Spieß, V. (1990): Pliocene-Pleistocene paleoceanography in the Weddell Sea - Siliceous microfossil evidence. - In Bleil, U. & Thiede, J. (Eds.) Geological History of the Polar Oceans: Arctic versus Antarctic. NATO/ASI Ser. C. Vol 308:729-760.

Abelmann, A., Bock, U., Gersonde, R., & Treppke, U. (in prep): A revised preparation technique for siliceous microfossils.

Anonymous (1975): Proposals for a standardization of diatom terminology and diagnoses.- In: Simonsen, R. (ed.). Third Symp. on Recent and Fossil Marine Diatoms. Kiel. Nova Hedwigia Beih. 53:323-354.

Barker, P. F., Kennett, J. P., et al. (1988): Proc. ODP, Init. Repts., 113: College Station, TX (Ocean Drilling Program).

Barron, J. A. (1985): Miocene to Holocene planktic diatoms. In: Bolli, H. M., Saunders, J. B., and K. Perch-Nielsen (eds.), Plankton Stratigraphy: Cambridge (Cambridge Univ. Press), 763-809.

Baldauf, J. G. & Barron, J. A. (in press): Diatom biostratigraphy: Kerguelen Plateau and Prydtz Bay regions of the Southern Ocean.- In: Barron, J. A., Schlich, R., et al., Proc. ODP, Sci. Results, 119:College Station, TX (Ocean Drilling Program).

Berggren, W. A., Kent, D. V. & Van Couvering, J. A., 1985: The Neogene: Part 2, Neogene geochronology and chronostratigraphy. - In: Snelling, N. J. (Ed.) Geochronology of the geological record. Geol. Soc. Mem. 10:211-260.

Brady, H. T. (1977): *Thalassiosira torokina* n. sp. (diatom) and its significance in Late Cenozoic biostratigraphy.- Antarctic J. U.S..12:122-123.

Ciesielski, P. F. (1983): The Neogene and Quaternary diatom biostratigraphy of Subantarctic sediments. Deep Sea Drilling Project Leg 71.- In: Ludwig, W. J., Krasheninnikov, V. A. , et al., Init. Repts. DSDP.71: Washington (U.S. Govt. Printing Office), 635-665.

Donahue, J. G. (1970): Diatoms as Quaternary biostratigraphic and paleoclimatic indicators in high-latitudes of the Pacific Ocean.- PhD thesis, Faculty of Pure Science, Columbia University, NY (unpublished manuscript).

Frenguelli, J. (1949): Diatomeas fosiles de los yacimientos chilenos de Tiltil y Mejiliones.- Darwiniana, 9 (1):97-156.

Fryxell, G. A. & Hasle, G. R. (1979): The genus *Thalassiosira*: species with internal extensions of the strutted precesses.- Phycologia. 18 (4):378-393.

Gersonde, R. (1990): Taxonomy and morphostructure of Neogene diatoms from the Southern Ocean, ODP Leg 113.- In: Barker, P. F., Kennett, J. P., et al, Proc. ODP, Sci. Results, 113:College Station, TX (Ocean Drilling Program) 791–802.

Gersonde, R. & Burckle, L. H. (1990): Neogene diatom biostratigraphy (ODP Leg 113). - In: Barker, P. F., Kennett, J. P., et al, Proc. ODP, Sci. Results, 113:College Station, TX (Ocean Drilling Program) 761–789.

Gersonde, R., Abelmann, A., Burckle, L. H., Hamilton, N., Lazarus, D., McCartney, K., O´Brien, B., Spieß, V., & Wise, S. W. (1990): Biostratigraphic synthesis of Neogene siliceous microfossils from the Antarctic Ocean, ODP Leg 113 (Weddell Sea). - In: Barker, P. F., Kennett, J. P., et al, Proc. ODP, Sci. Results, 113:College Station, TX (Ocean Drilling Program) 915–936.

Plate 1: All specimens at x 1,500 unless otherwise indicated: **1 - 6, 26:** *Nitzschia lacrima* sp. nov., Sample PS1467-1, 866 cm, (1, 4) paratypes, (2 - 3) holotype, (26) SEM oblique outside view on valve margin and raphe, bar = 10 µm. **7 - 17:** *Nitzschia praecurta* sp. nov., (10) paratype, Sample PS1467-1, 790 cm, (11) holotype, Sample PS1467-1, 790 cm, (7, 9, 12, 14) Sample PS1467-1, 804 cm, (8, 13, 15 - 16) Sample PS1467-1, 800 cm, (17) Sample PS1467-1, 816 cm. **18 - 25:** *Nitzschia aurica* sp. nov., (19) holotype, Sample PS1467-1, 804 cm, (20) paratype, Sample PS1467-1, 804 cm, (18, 23 - 25) Sample PS1467-1, 804 cm, (21 - 22) Sample PS1467-1, 811 cm.

Tafel 1: Vergrößerung x 1.500, außer wenn anders angegeben: **1 - 6, 26:** *Nitzschia lacrima* sp. nov., Probe PS1467-1, 866 cm, (1, 4) Paratypen, (2 - 3) Holotypus, (26) REM Außenansicht auf Schalenrand und Raphe. Maßstab = 10 µm. **7 - 17:** *Nitzschia praecurta* sp. nov., (10) Paratypus , Probe PS1467-1, 790 cm, (11) Holotypus, Probe PS1467-1, 790 cm, (7, 9, 12, 14) Probe PS1467-1, 804 cm, (8, 13, 15 - 16) Probe PS1467-1, 800 cm, (17) Probe PS1467-1, 816 cm. **18 - 25:** *Nitzschia aurica* sp. nov., (19) Holotypus, Probe PS1467-1, 804 cm, (20) Paratypus, Probe PS1467-1, 804 cm, (18, 23 - 25) Probe PS1467-1, 804 cm, (21 - 22) Probe PS1467-1, 811 cm.

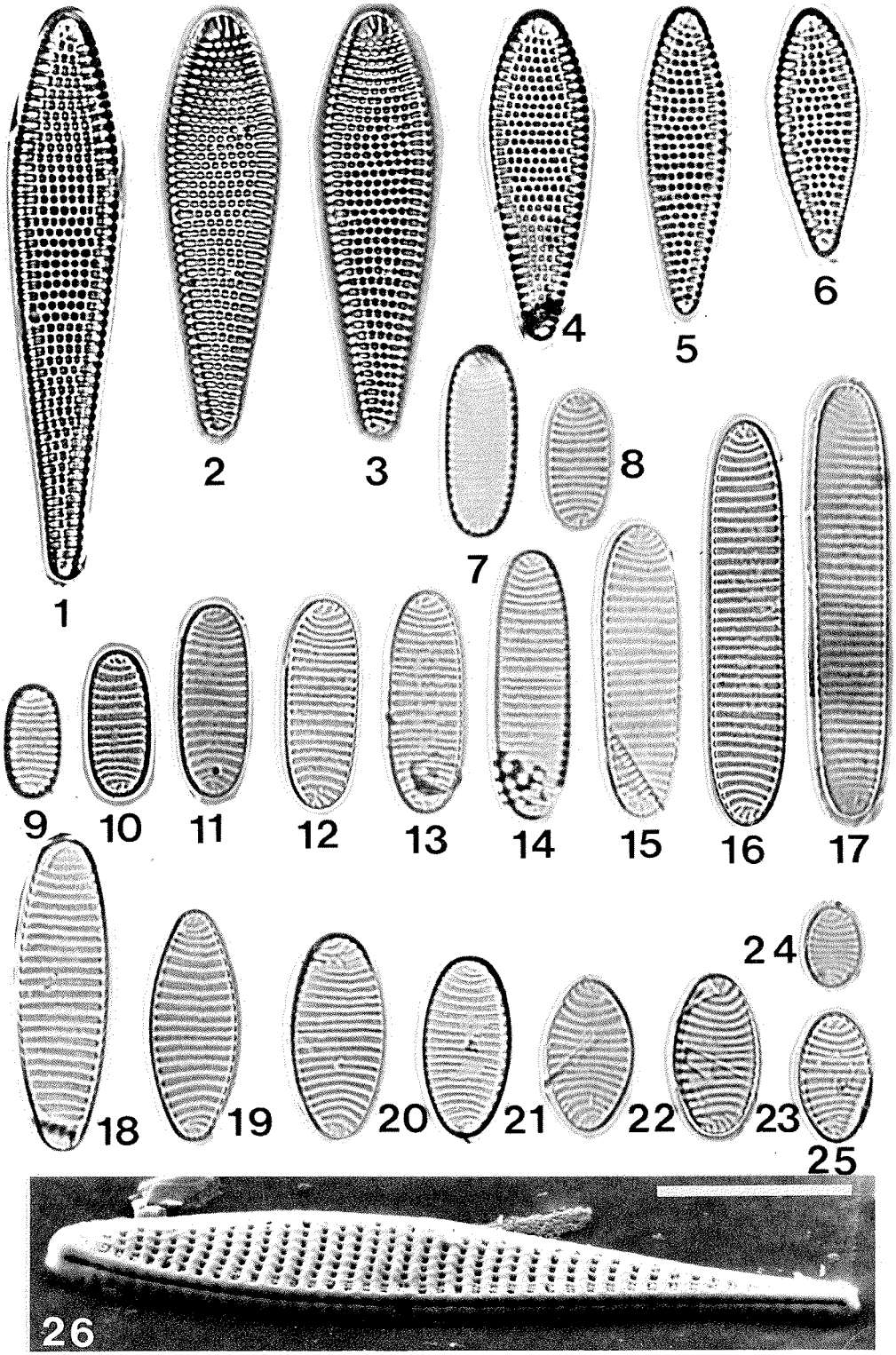
1
2
3
4
5
6
7
8
9
10
11
12
13
14
15
16
17
18
19
20
21
22
23
24
25
26

Gombos, A. M. (1974): New species of fossil diatom from the Antarctic.- Antarctic J. U.S., 9:275.

Gombos, A. M. (1977): Paleogene and Neogene diatoms from the Falkland Plateau and Malvinas Outer Basin: Leg 36, Deep Sea Drilling Project. - In: Barker, P. F., Dalziel, I. W. D. et al., Init. Repts. DSDP, 36: Washington (U.S. Govt. Printing Office),575-687.

Gombos, A. M. & Ciesielski, P. F. (1983): Late Eocene to early Miocene diatoms from the Southwest Atlantic.- In: Ludwig, W. J., Krasheninnikov, V. A. et al., Init. Repts. DSDP, 71: Washington (U.S. Govt. Printing Office),583-634.

Greuter, W. et al. (1988): International Code of Botanical Nomenclature.- Koeltz, Königstein, 328 p.

Hasle, G. R. (1964): *Nitzschia* and *Fragilariopsis* species studied in the light and electron microscopes. I. Some marine species of the groups Nitzschiella and Lanceolatae. - Skr. Norsk Vidensk-Akad. Oslo I. Mat.-Nat. Kl., Ny Ser. 16:1-48, 16 plates.

Hasle, G. R. (1965a): *Nitzschia* and *Fragilariopsis* species studied in the light and electron microscopes. II. The groups Pseudonitzschia. - Skr. Norsk Vidensk-Akad. Oslo I. Mat.-Nat. Kl., Ny Ser. 18:1-45, 17 plates.

Hasle, G. R. (1965b): *Nitzschia* and *Fragilariopsis* species studied in the light and electron microscopes. III. The genus *Fragilariopsis*. - Skr. Norsk Vidensk-Akad. Oslo I. Mat.-Nat. Kl., Ny Ser. 21:1-49, 17 plates.

Hasle, G. R. (1973a): Thalassiosiraceae, a new diatom family.- Norw. J. Bot., 20:67-69.

Hasle, G. R. (1973b): Some marine plankton genera of the diatom family Thalassiosiraceae.- Nova Hedwigia, Beih. 45:1-67.

Hasle, G. R. (1974): Validation of the names of some marine planktonic species of *Nitzschia* (Bacillariophyceae).- Taxon 23(2/3):425-428.

Hasle, G. R. & Booth, B. C. (1984): *Nitzschia cylindroformis* sp. nov., a common and abundant nanoplankton diatom of the eastern subarctic Pacific.- J. Plankton Res., Vol. 6:493-503.

Heiden, H. & Kolbe, R. W. (1928): Die marinen Diatomeen der Deutschen Südpolarexpedition 1901-1903.- In: Drygalski, E. von (Ed.), Deutsche Südpolar-Expedition (1901-1903), Bd. 8, Botanik: Berlin und Leipzig, 58 - 708, 193 figs.

Hendey, N. I. (1981): Miocene diatoms from the Subantarctic southwest Pacific, Deep Sea Drilling Project Leg 29, Sites 278, Core 10. - Bacillaria, 4:65-124.

Johansen, J. R. & Fryxell, G. A. (1985): The genus *Thalassiosira* (Bacillariophyceae): studies on species occurring south of the Antarctic Convergence Zone.- Phycologia, 24:155-179.

Jousé, A. P., Koroleva, G. S. & Nagaeva, G. A. (1962): Diatoms in the surface layer of sediment in the Indian sector of the Antarctic.- Trudi Inst. Okeanol. Akad. NAUK, SSSR, 61:20-101 (in Russian with English summary).

Koizumi, I. (1980): Neogene diatoms from the Emperor Seamount Chain, Leg 55, Deep Sea Drilling Project. - In: Jackson, E. D., Koizumi, I., et al., Init. Repts. DSDP,55: Washington (U.S. Govt. Printing Office), 387-407.

McCollum, D. W. (1975): Diatom stratigraphy of the Southern Ocean.- In Hayes, D. E., Frakes, L. A., et al., Init. Repts. DSDP, 28: Washington (U.S. Govt. Printing Office), 515-571.

Ross, R., Cox, E. J., Karayeva, N. J., Mann, D. G., Paddock, T. B. B., Simonsen, R. & Sims, P. A. (1979): An amended terminology for the siliceous components of the diatom cell.- Nova Hedwigia, Beih., 64:513-533.

Schrader, H. J. (1976): Cenozoic planktonic diatom biostratigraphy of the Southern Pacific Ocean.- In: Hollister, C. D., Craddock, C., et al., Init. Repts. DSDP,35: Washington (U.S. Govt. Printing Office), 605-671.

Schrader, H. J. & Fenner, J. (1976): Norwegian Sea Cenozoic diatom biostratigraphy and taxonomy, Part 1, Norwegian Sea Cenozoic diatom biostratigraphy. - In: Talwani, M., Udintsev, G., et al., Init. Repts. DSDP,38: Washington (U.S. Govt. Printing Office), 921-1099.

Spieß, V. (1990): Cenozoic magnetostratigraphy of ODP Leg 113 drill sites on Maud Rise, Weddell Sea, Antarctica.- In: Barker, P. F., Kennett, J. P., et al. Proc. ODP, Sci. Results, 113:College Station, TX (Ocean Drilling Program) 261-315.

Sundström, B. G. (1986): The marine diatom genus Rhizosolenia. PhD dissertation, Lund University, 196 p.

Weaver, F. M & Gombos, A. M. (1981): Southern High-Latitude diatom biostratigraphy. - Soc. Econ. Paleontol. Mineral. Spec. Publ. 32:445-470.

Plate 2: Scale bar = 10 µm; **1 - 3:** *Nitzschia lacrima* sp. nov., Sample PS1467-1, 866 cm (1 - 2) outside view of same specimen as in Pl. 1, Fig. 26, (3) oblique inside view. **4:** *Nitzschia arcula* sp. nov., inside view, Sample PS1467-1, 1050 cm. **5 - 6:** *Nitzschia praecurta* sp. nov., inside view, easily discernible fibulae and strial structure, (5) Sample PS1467-1, 760 cm, (6) Sample PS1467-1, 800 cm.

Tafel 2: Maßstab = 10 µm; **1 - 3:** *Nitzschia lacrima* sp. nov., Probe PS1467-1, 866 cm (1 - 2) Außenansicht der gleichen Schale wie in Taf. 1, Abb. 26, Fig. 26, (3) Innenansicht. **4:** *Nitzschia arcula* sp. nov., Innenansicht, Probe PS1467-1, 1050 cm. **5 - 6:** *Nitzschia praecurta* sp. nov., Innenansicht, deutlich erkennbar Fibulae und Aufbau der Striae, (5) Probe PS1467-1, 760 cm, (6) Probe PS1467-1, 800 cm.

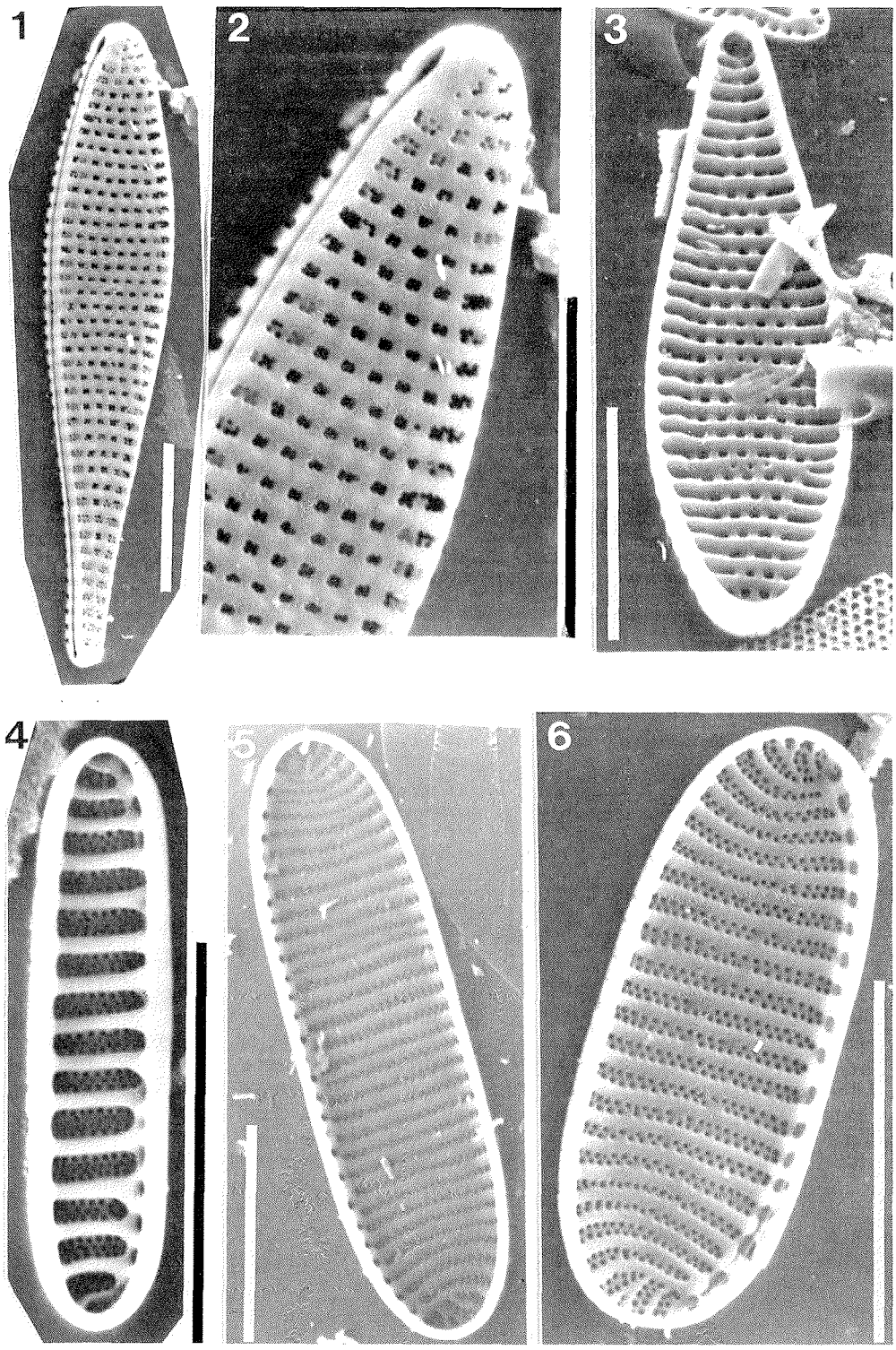
1
2
3
4
5
6

Plate 3: Scale bar = 10 µm: **1 - 2:** *Thalassiosira complicata* sp. nov., outside view of valve face with median ring of strutted processes, central hyaline area and outer opening of labiate process (arrow), Sample PS1467-1, 200 cm. **3 - 4:** *Nitzschia praecurta* sp. nov., (3) oblique outside view on raphe, Sample PS1467-1, 700 cm, (4) outside view of valve face, Sample PS1467-1, 600 cm. **5:** *Nitzschia aurica* sp. nov., outside view of valve face, Sample PS1467-1, 600 cm. **6:** *Nitzschia barronii* sp.nov., outside view of valve face, Sample PS1467-1, 200 cm.

Tafel 3: Maßstab = 10 µm: **1 - 2:** *Thalassiosira complicata* sp. nov., Außenansicht der Schalenfläche mit medianem Ring von Stützfortsätzen, hyaliner Zentralarea und äußerer Öffnung des Lippenfortsatzes (Pfeil), Probe PS1467-1, 200 cm. **3 - 4:** *Nitzschia praecurta* sp. nov., (3) Außenansicht mit Raphe, Probe PS1467-1, 700 cm, (4) Außenansicht der Schalenfläche, Probe PS1467-1, 600 cm. **5:** *Nitzschia aurica* sp. nov., Außenansicht der Schalenfläche, Probe PS1467-1, 600 cm. **6:** *Nitzschia barronii* sp.nov., Außenansicht der Schalenfläche, Probe PS1467-1, 200 cm.

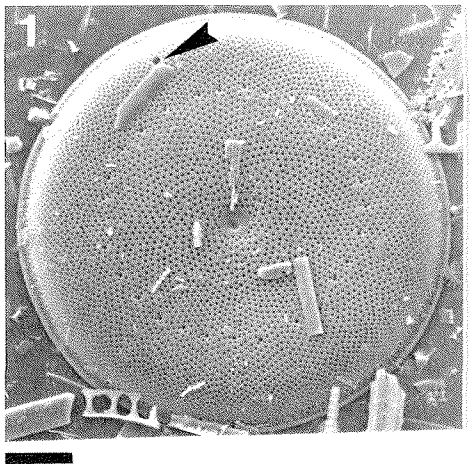
1

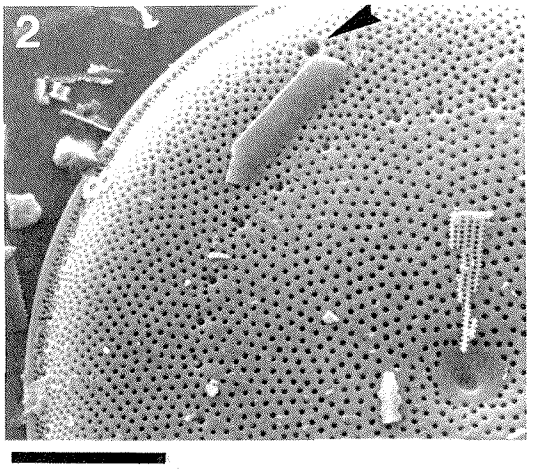
2

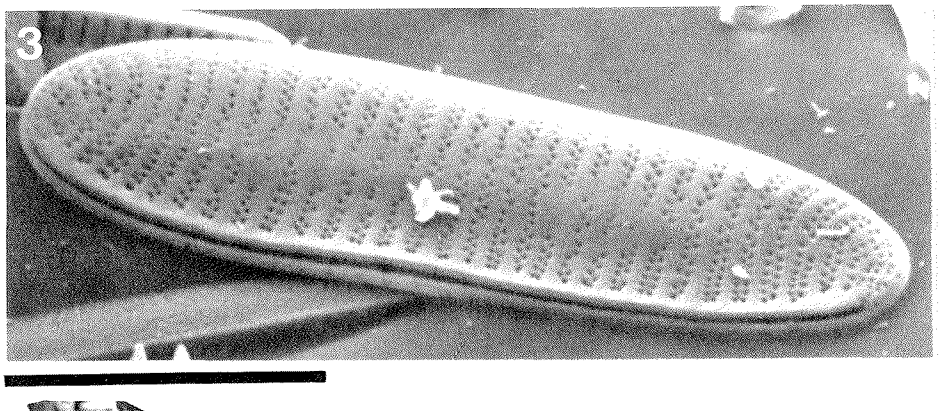
3

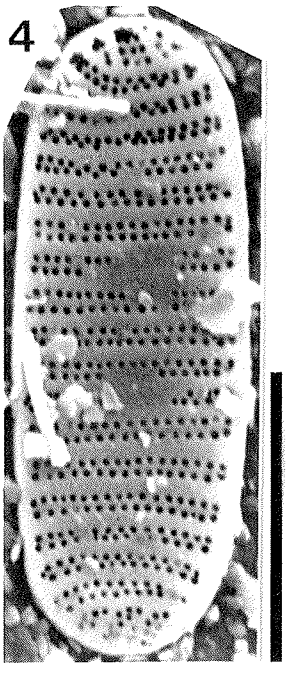
4

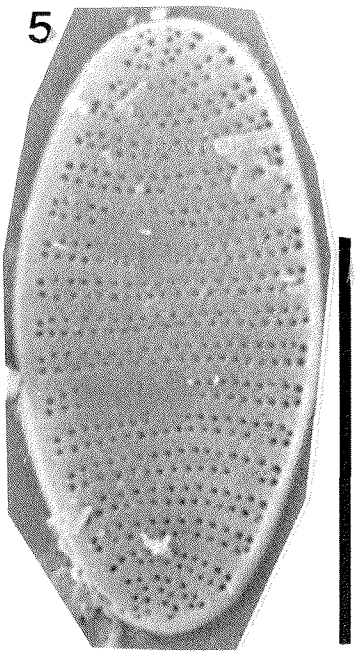
5

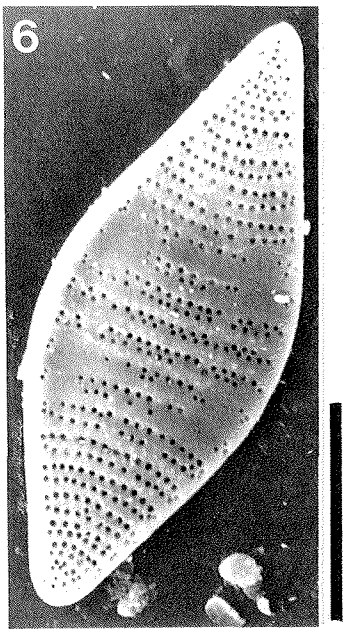
6

Plate 4: Scale bar = 10 µm unless otherwise indicated; **1 - 3:** *Nitzschia barronii* sp. nov., (1) outside view of valve face, marginal raphe easily discernible Sample PS1467-1, 200 cm, (2 - 3) Inside view of valve face, Sample PS1467-1, 200 cm. **4:** *Nitzschia arcula* sp. nov., outside view of valve face, marginal raphe well discernable, Sample PS1467-1, 804 cm. **5 - 6:** *Nitzschia aurica* sp. nov., inside view of valve face, (5) corroded valve, Sample PS1467-1, 600 cm, (6) Sample PS1467-1, 1090 cm, bar = 1 µm.

Tafel 4: Maßstab = 10 µm, außer wenn anders angegeben; **1 - 3:** *Nitzschia barronii* sp. nov., (1) Außenansicht der Schalenfläche, randliche Raphe gut erkennbar, Probe PS1467-1, 200 cm, (2 - 3) Innenansicht, Probe PS1467-1, 200 cm. **4:** *Nitzschia arcula* sp. nov., Außenansicht der Schalenfläche, randliche Raphe gut erkennbar, Probe PS1467-1, 804 cm. **5 - 6:** *Nitzschia aurica* sp. nov., Innenansicht der Schalenfläche, (5) angelöste Schale, Probe PS1467-1, 600 cm, (6) Probe PS1467-1, 1090 cm, Maßstab = 1 µm.

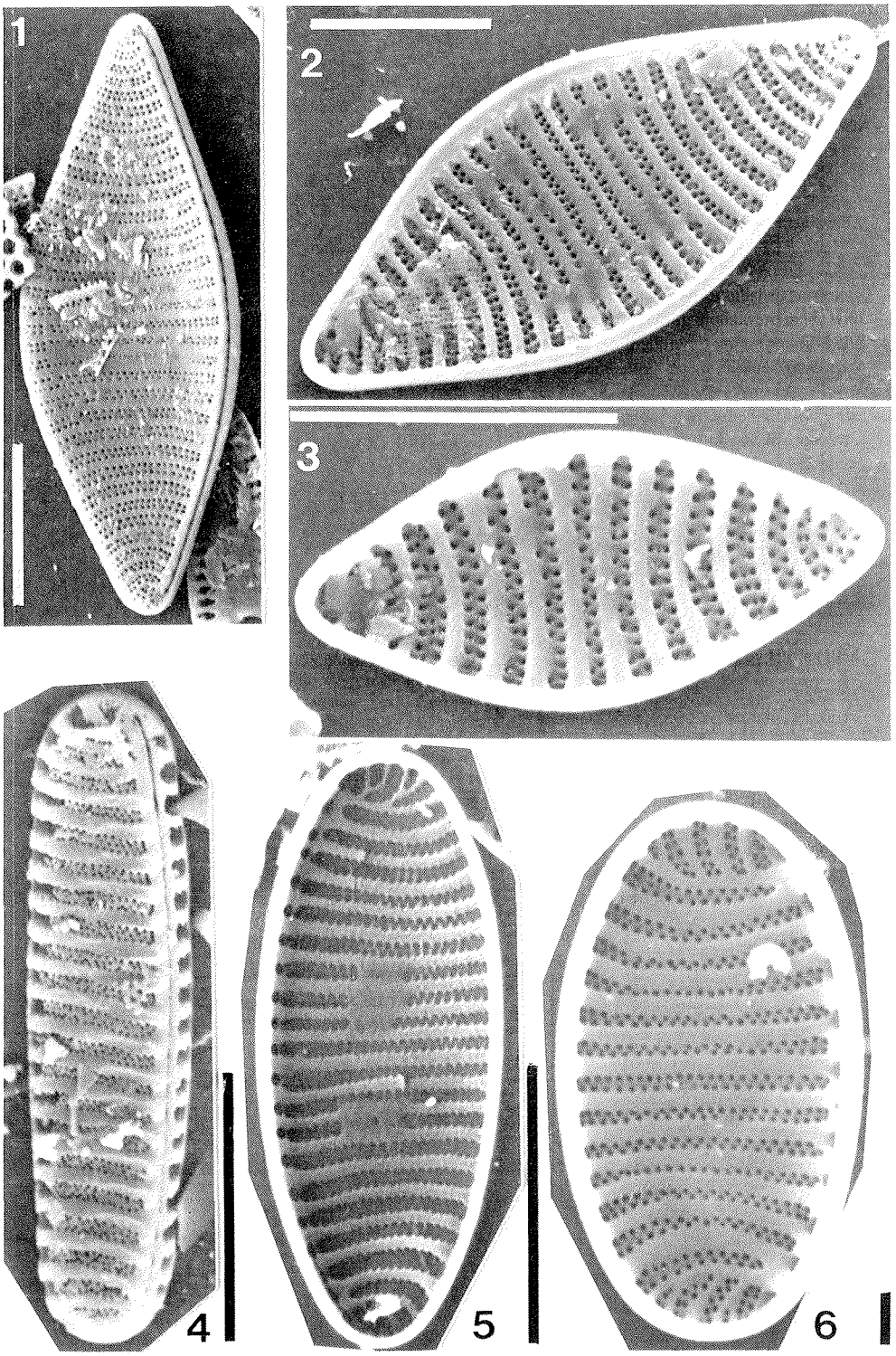
1
2
3
4
5
6

Plate 5: All specimens at x 1,500: **1 - 6:** *Nitzschia arcula* sp. nov., (1) holotype, Sample PS1467-1, 804 cm, (2) Sample PS1467-1, 811 cm, (3) paratype, Sample PS1467-1, 804 cm, (4 - 6) Sample PS1467-1, 804 cm. **7 - 17:** *Nitzschia barronii* sp. nov., Sample PS1467-1, 200 cm (13), paratype, (14) holotype. **18 - 20:** *Thalassiosira complicata* sp. nov., (18) labiate process indicated by arrow, Sample PS1467-1, 800 cm, (19 - 20) single specimen at different focus, Sample PS1467-1, 200 cm. **21:** *Nitzschia* sp. A, Sample PS1467-1, 200 cm.

Tafel 5: Vergößerung x 1,500: **1 - 6:** *Nitzschia arcula* sp. nov., (1) Holotypus, Probe PS1467-1, 804 cm, (2) Probe PS1467-1, 811 cm, (3) Paratypus, Probe PS1467-1, 804 cm, (4 - 6) Probe PS1467-1, 804 cm. **7 - 17:** *Nitzschia barronii* sp. nov., Probe PS1467-1, 200 cm, (13) Paratypus, (14) Holotypus. **18 - 20:** *Thalassiosira complicata* sp. nov., (18) Lippenfortsatz durch Pfeil markiert, Probe PS1467-1, 800 cm, (19 - 20) Schale bei unterschiedlicher Fokussierung, Probe PS1467-1, 200 cm. **21:** *Nitzschia* sp. A, Probe PS1467-1, 200 cm.

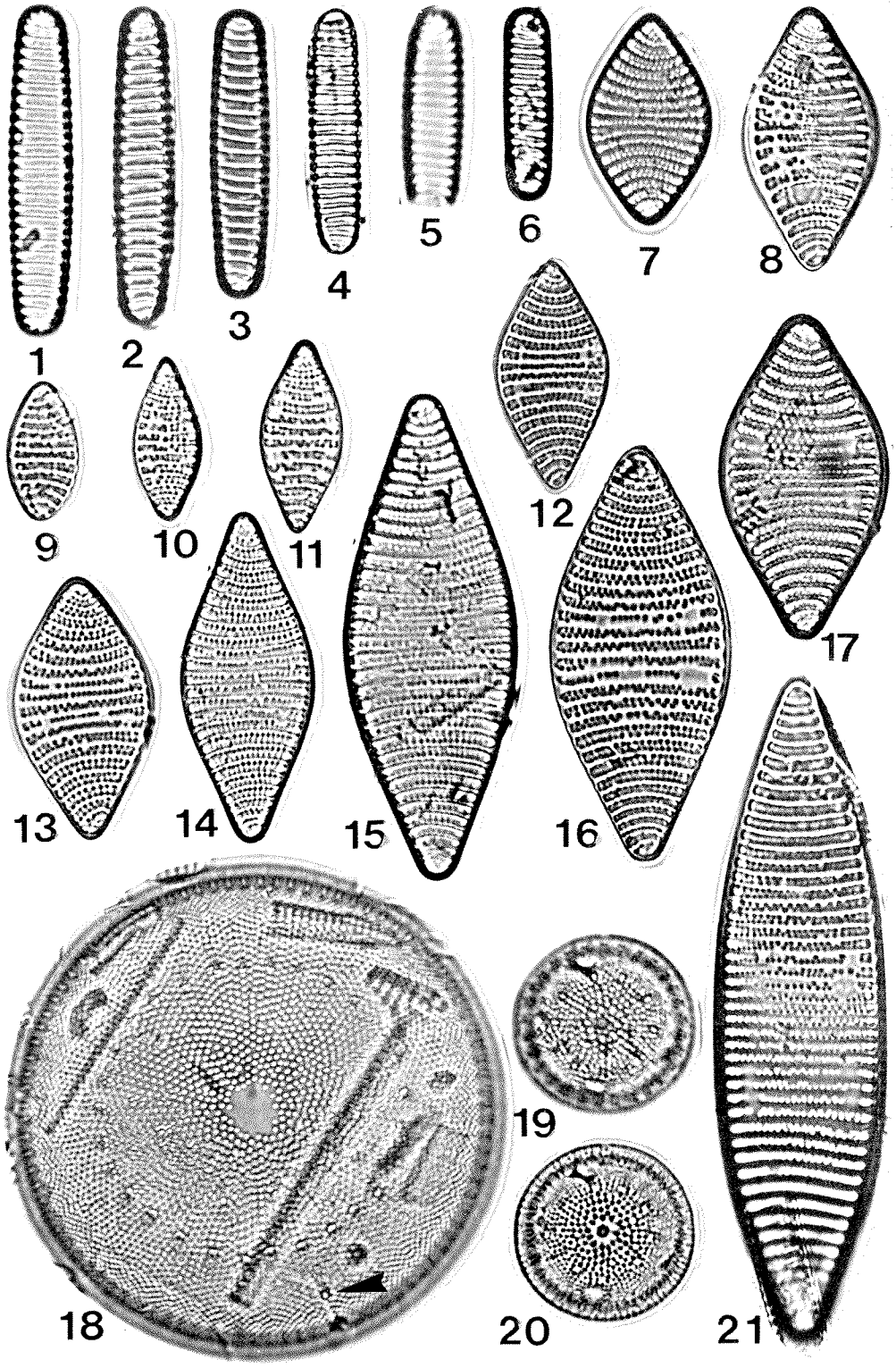
1
2
3
4
5
6
7
8
9
10
11
12
13
14
15
16
17
18
19
20
21

Plate 6: All specimens at x 1,500: **1 - 6:** *Thalassiosira complicata* sp. nov., (1 - 3) holotype at different focus, labiate process indicated by arrow, Sample PS1467-1, 200 cm, (4 - 5) paratype at different focus, Sample PS1467-1, 200 cm, (6) Sample PS1467-1, 800 cm, **7 - 14:** *Thalassiosira inura* sp. nov., Sample PS1467-1, 200 cm, (7 - 8) holotype at different focus, (9 - 10) paratype at different focus, (12 - 13) same specimen at different focus.

Tafel 6: Vergößerung x 1,500: **1 - 6:** *Thalassiosira complicata* sp. nov., (1 - 3) Holotypus bei unterschiedlicher Fokussierung, Lippenfortsatz durch Pfeil markiert, Probe PS1467-1, 200 cm, (4 - 5) Paratypus bei unterschiedlicher Fokussierung, Probe PS1467-1, 200 cm, (6) Probe PS1467-1, 800 cm, **7 - 14:** *Thalassiosira inura* sp. nov., Probe PS1467-1, 200 cm, (7 - 8) Holotypus bei unterschiedlicher Fokussierung, (9 - 10) Paratypus bei unterschiedlicher Fokussierung, (12 - 13) bei unterschiedlicher Fokussierung.

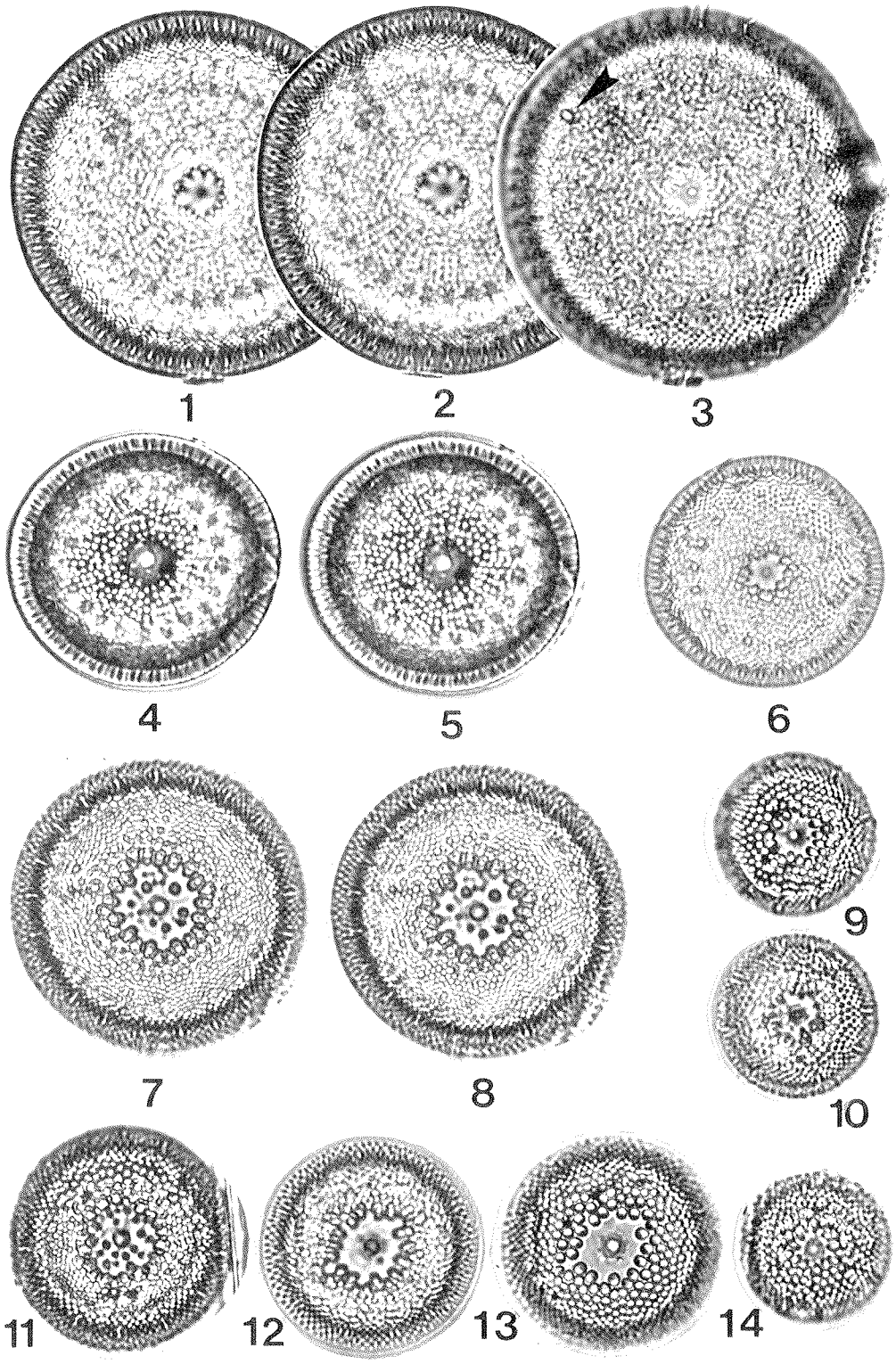
1
2
3
4
5
6
7
8
9
10
11
12
13
14

Plate 7: Scale bar = 10 µm unless otherwise indicated; **1 - 5:** *Thalassiosira complicata* sp. nov., (1) oblique inside view of valve face, labiate process indicated by arrow, Sample PS1467-1, 700 cm, (2) outside view of valve face, outer opening of labiate process indicated by arrow, Sample PS1467-1, 866 cm, (3) close up of specimen in (1) with median and marginal strutted processes with small internal extensions and opercula covering the four satellite pores, bar = 5 µm, (4) oblique outside view of specimen in (2), (5) broken valve showing cross-section of areolae with cylindriform structure of areolae chambers, Sample PS1467-1, 200 cm. **6:** *Nitzschia aurica* sp. nov., outside view of valve face with marginal raphe, Sample PS1467-1, 600 cm, bar = 1 µm.

Tafel 7: Maßstab = 10 µm, außer wenn anders angegeben; **1 - 5:** *Thalassiosira complicata* sp. nov., (1) Innenansicht der Schalenfläche, Lippenfortsatz durch Pfeil markiert, Probe PS1467-1, 700 cm, (2) Außenansicht der Schalenfläche, äußere Öffnung des Lippenfortsatzes durch Pfeil markiert, Probe PS1467-1, 866 cm, (3) Detail der Schale in (1) mit medianen und randlichen Stützfortsätzen mit kleinen internen Verlängerungen und Opercula über den vier Satellitenporen, Maßstab = 5 µm, (4) Außenansicht der Schalenfläche in (2), (5) gebrochene Schale mit Querschnitt der Areolae, deutlich erkennbar zylindrische Form der Areolenkammern, Probe PS1467-1, 200 cm, 6: *Nitzschia aurica* sp. nov., Außenansicht der Schalenfläche mit randlicher Raphe, Probe PS1467-1, 600 cm, Maßstab = 1 µm.

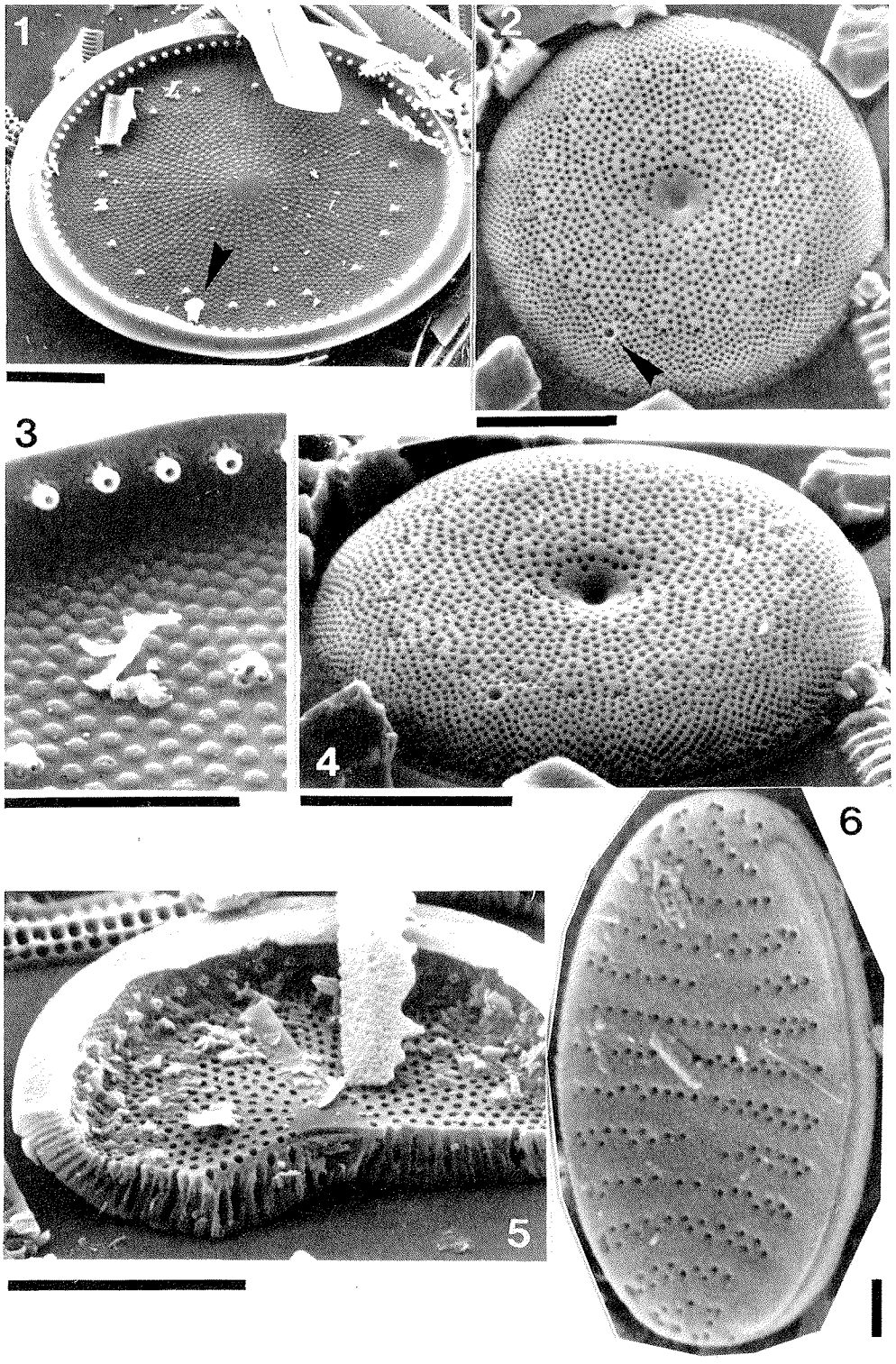
1
2
3
4
5
6

Plate 8: Scale bar = 10 µm; **1 - 6:** *Thalassiosira inura* sp. nov., (1) oblique outside view of valve face, outer opening of single median strutted process left arrow, opening of labiate process right arrow, Sample PS1467-1, 866 cm, (2) oblique inside view of valve face, easily discernible central hyaline area lacking processes, position of single labiate and strutted process and structure of strutted process with small internal extensions and opercula covering the four satellite pores, (3) outside view of valve face with central circular depression, Sample PS1467-1, 866 cm, (4) outside view of valve face, Sample PS1467-1, 800 cm, (5) oblique inside view of valve face, Sample PS1467-1, 700 cm, (6) broken valve showing cross-section of areolae with large bulbous inflated chambers in the central portion of valve and narrow cylindriform chambers near the margin, Sample PS1467-1, 800 cm.

Tafel 8: Maßstab = 10 µm; **1 - 6:** *Thalassiosira inura* sp. nov., (1) Außenansicht der Schalenfläche, linker Pfeil markiert äußere Öffnung des medianen Stützfortsatzes, rechter Pfeil markiert Öffnung des Lippenfortsatzes, Probe PS1467-1, 866 cm, (2) Innenansicht der Schalenfläche, gut erkennbar hyaline Zentralarea ohne Prozesse, die Anordnung des Lippenfortsatzes sowie der Stützfortsätze und deren Aufbau mit kleinen internen Verlängerungen und Opercula über den vier Satellitenporen, (3) Außenansicht der Schalenfläche mit runder Vertiefung im Zentrum, Probe PS1467-1, 866 cm, (4) Außenansicht der Schalenfläche, Probe PS1467-1, 800 cm, (5) Innenansicht der Schalenfläche, Probe PS1467-1, 700 cm, (6) gebrochene Schale mit Querschnitt der Areolae, deutlich erkennbar die aufgeblähte Form der Areolenkammern im mittleren Bereich der Schale und die schmale, zylindrische Form der Kammern im Randbereich, Probe PS1467-1, 800 cm.

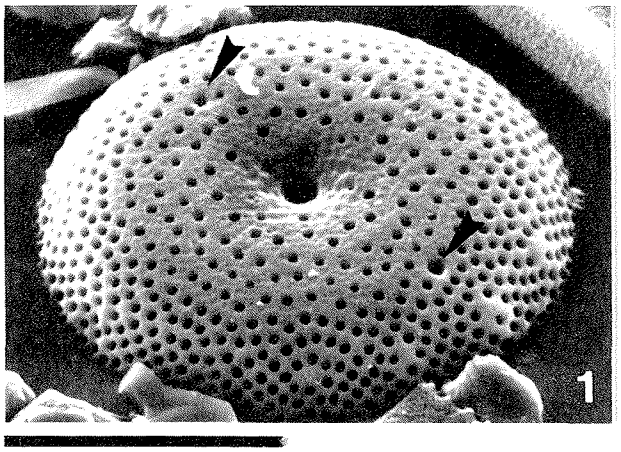
1

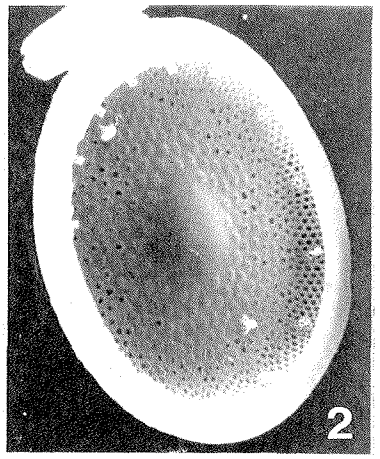
2

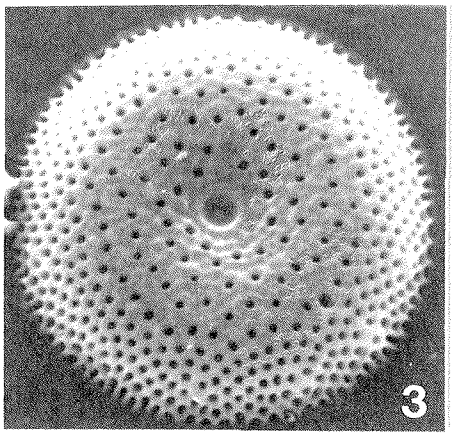
3

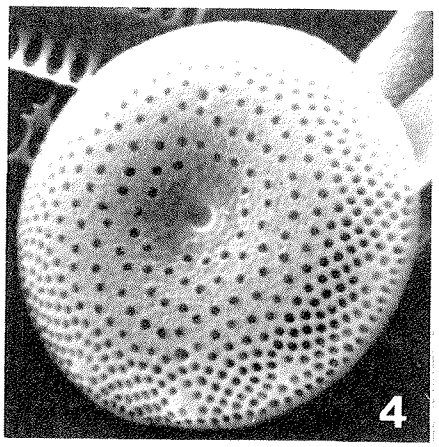
4

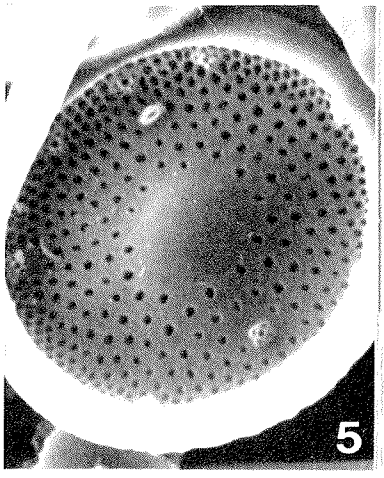
5

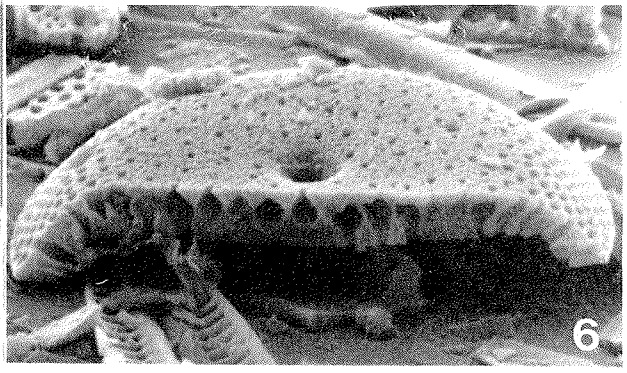
6

Plate 9: All specimens at x 1,500; **1 - 6:** *Rhizosolenia costata* sp. nov., (1 - 3) holotype at different focus, Sample PS1467-1, 970 cm, (3 - 6) paratype at different focus, Sample PS1467-1, 970 cm.

Tafel 9: Vergößerung x 1.500; **1 - 6:** *Rhizosolenia costata* sp. nov., (1 - 3) Holotypus bei unterschiedlicher Fokussierung, Probe PS1467-1, 970 cm. (3 - 6) Paratypus bei unterschiedlicher Fokussierung, Probe PS1467-1, 970 cm.

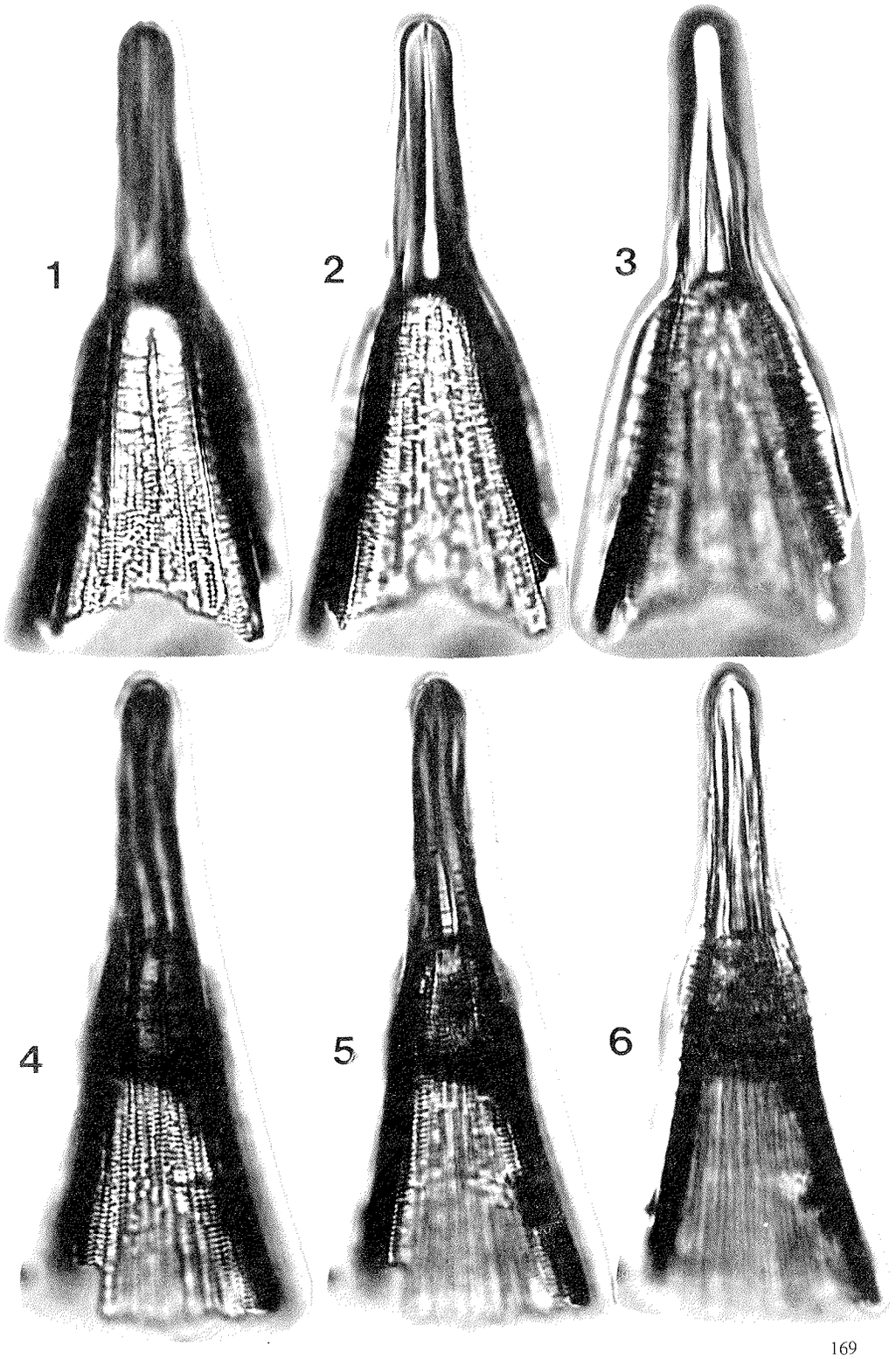
1
2
3
4
5
6

Plate 10: Scale bar = 10 µm unless otherwise indicated; **1 - 6:** *Rhizosolenia costata* sp. nov., (1) oblique view of valve, Sample PS1467-1, 800 cm, bar = 100 µm, (2) close up of inside of basal valve portion of specimen in (1), (3) outside view, Sample PS1467-1, 760 cm, (4 - 5) outside views, showing costae walls strutted by tangentially oriented thickenings, Sample PS1467-1, 700 cm, (6) process with outer opening of specimen in (3). **7:** *Nitzschia praecurta* sp. nov., outside view of valve face, Sample PS1467-1, 760 cm, bar = 5 µm.

Tafel 10: Maßstab = 10 µm, außer wenn anders angegeben; **1 - 6:** *Rhizosolenia costata* sp. nov., (1) Außenansicht der Schalenfläche, Probe PS1467-1, 800 cm, Maßstab = 100 µm, (2) Detail der Innenstruktur an der Basis der Schale in (1), (3) Außenansicht, Probe PS1467-1, 760 cm, (4 - 5) Außenansicht mit Costae, die durch tangential angeordnete Verdickungen gestützt werden, Probe PS1467-1, 700 cm, (6) Prozess mit äußerer Öffnung der Schale in (3). **7:** *Nitzschia praecurta* sp. nov., Außenansicht der Schalenfläche, Probe PS1467-1, 760 cm, Maßstab = 5 µm.

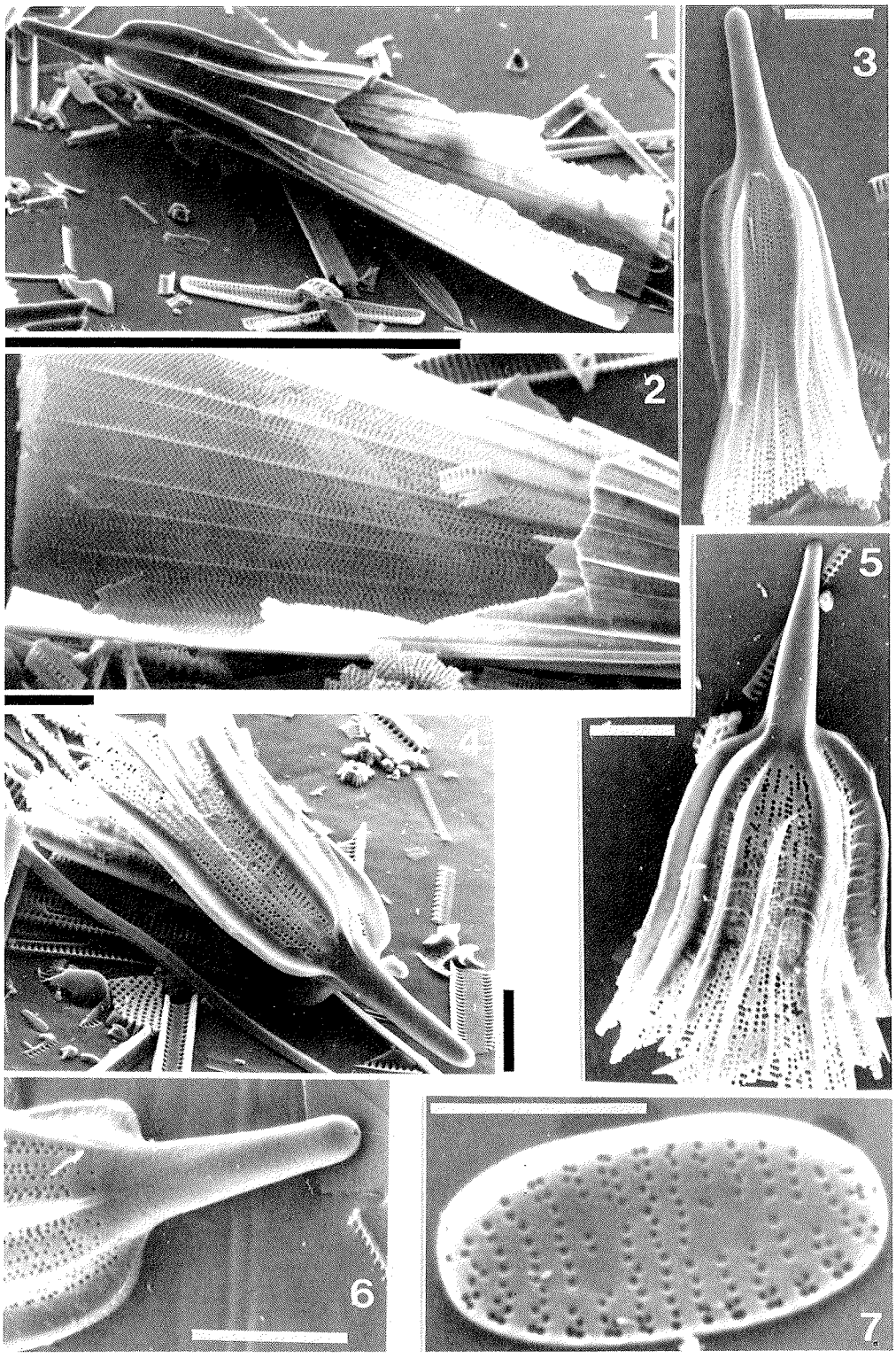
1
2
3
4
5
6
7